Substrate-Dependent Effects on the Conformational Equilibrium of the Na$^+$,K$^+$-ATPase monitored by VCF

Dissertation

zur Erlangung des Doktorgrades

der Naturwissenschaften

vorgelegt beim Fachbereich Biochemie, Chemie, Pharmazie

der Johann Wolfgang Goethe – Universität

in Frankfurt am Main

von

Stefan Geys

aus Würzburg

Frankfurt 2008

D30

Vom Fachbereich Biochemie, Chemie, Pharmazie der

Johann Wolfgang Goethe – Universität als Dissertation angenommen.

Dekan: ………………………………………………………………………………….

Gutachter: …………………………………………………………………………………

Datum der Disputation: …………………………………………………………………...

Meinen Eltern

Abstract

The Na^+,K^+-ATPase was discovered more than 50 years ago, but even today the pump-cycle and its partial reactions are still not completely understood. In this thesis, Voltage Clamp Fluorometry was used to monitor the conformational changes that are associated with several electrogenic partial reactions of the Na^+,K^+-ATPase. The conformational dynamics of the ion pump were analyzed at different concentrations of internal Na^+ or of external K^+ and the influences on the conformational equilibrium were determined. To probe the effect of the internal Na^+ concentration on the Na^+ branch of the ion pump, oocytes were first depleted of internal Na^+ and then loaded with Na^+ using the epithelial sodium channel which can be blocked by amiloride. The conformational dynamics of the K^+ branch were studied using different external K^+ concentrations in the presence and in the absence of external Na^+ to yield additional information on the apparent affinity of K^+.

The results of our Voltage Clamp Fluorometry experiments demonstrate that lowering the intracellular concentration of Na^+ has a comparable effect on the conformational equilibrium as increasing the amount of K^+ in the external solution. Both of these changes shift the equilibrium towards the $E_1/E_1(P)$ conformation. Furthermore, it can be shown that the ratio between external Na^+ and K^+ ions is also a determinant for the position of the conformational equilibrium: in the absence of external Na^+, the K^+ dependent shift of the equilibrium towards E_1 was observed at a much lower K^+ concentration than in the presence of Na^+. In addition, indications were found that both external K^+ and internal Na^+ bind within an ion well. Finally, the crucial role of negatively charged glutamate residues in the 2nd extracellular loop for the control of ion-access to the binding sites could be verified.

Table of contents

1. Introduction

The Na^+,K^+-ATPase, discovered in 1957 by Jens Skou (Skou, 1957), is a P-type ATPase that is expressed in almost all animal cells. It is a cation transporter that maintains a low intracellular Na^+ concentration and a high intracellular K^+ concentration against the prevalent ion gradients. This is achieved by phosphorylation of the pump by ATP during the transport cycle. The Na^+,K^+-ATPase plays a predominant role in electrolyte and fluid balance and is especially important in the excitable cells of heart, muscle and brain as well as for the reabsorbtion of Na^+ in the kidney. Lately, the possible involvement of the pump in cell signalling and cell motility as well as cancer progression have also made it an interesting candidate for drug targeting (Aperia, 2007; Kaplan, 2005).

1.1 The Na^+,K^+-ATPase

1.1.1 Structure of the Na^+,K^+-ATPase

Recently, an X-ray crystal structure of the Na^+,K^+-ATPase at a resolution of 3.5 Å has become available (Fig. 1.1, Morth et al., 2007). The present structure represents the pig renal Na^+,K^+-ATPase $\alpha\beta\gamma$ heterotrimer with bound K^+/Rb^+ counterions (i.e. the $E_2 \cdot P$-$2K^+$ conformation). In addition, structural information of several different conformations is available for the homologous single subunit P-type ATPase SERCA (sarco(endo)plasmic reticulum Ca^{2+} ATPase) that also provide valuable information about the sodium pump (Olesen et al., 2007).
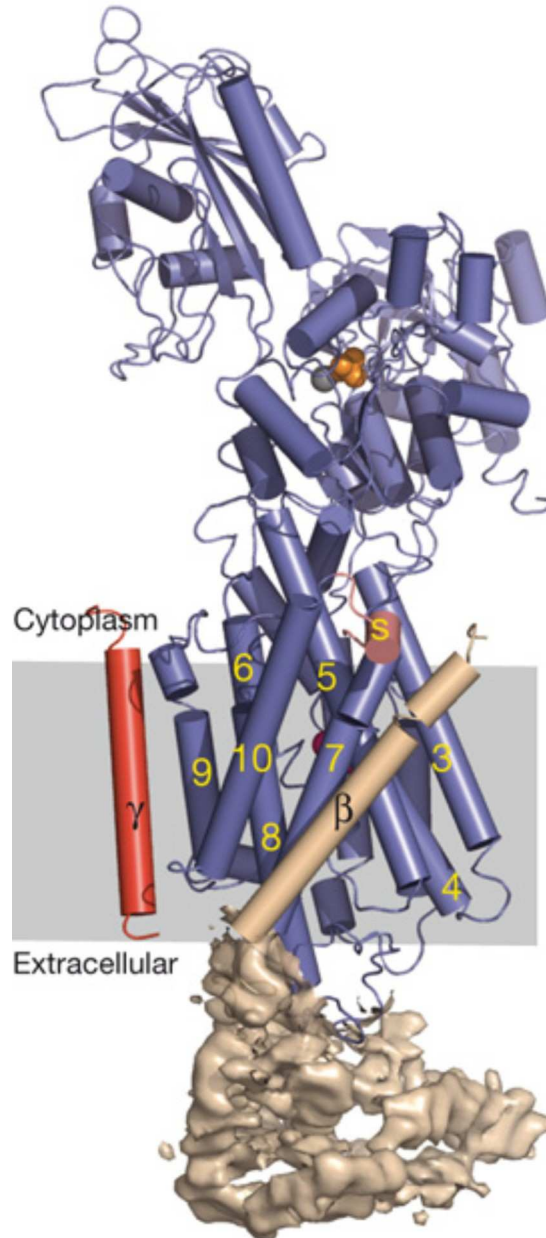
Fig. 1.1: Structure of the Na$^+$,K$^+$-ATPase αβγ heterotrimer (blue, wheat, red) with bound K$^+$/Rb$^+$ counterions. The transmembrane segments of the α subunit are numbered 1-10 starting at the N-terminus. S denotes the small C-terminal helix switch. Mg^{2+}, MgF$_4^{2-}$ and Rb$^+$ ions (grey, orange, pink) are shown. Taken from Morth et al., 2007.

Characterization of the Na$^+$,K$^+$-ATPase subunits

The Na$^+$,K$^+$-ATPase consists of a α/β heterodimer which is often associated with another subunit from the FXYD protein family (Morth et al., 2007). Whereas the α-subunit is the major catalytic subunit, the β-subunit is responsible for stabilisation, proper trafficking to

the plasma membrane and modulation of cation affinities (Jorgensen et al., 2003). Several tissue and cell-specific isoforms of both subunits have been identified. The FXYD protein family represents a group of small, regulatory membrane proteins such as the γ-subunit (Geering, 2005).

The α-subunit: In homology to SERCA, the α-subunit consists of a bundle of ten transmembrane helices that contribute the pathway for cation transport. Whereas the loop region on the extracellular side is rather inconspicuous, three functionally important cytoplasmic domains can be identified: the A (actuator), P (phosphorylation) and N (nucleotide binding) domain (Morth et al., 2007).

Different functions can be attributed to these domains: The N domain stretches from the phosphorylation site to the C-terminal hinge and allows for ATP binding. The P domain contains the conserved DKTGT motif with the aspartate residue that is transiently phosphorylated during the pump cycle. The A domain contains the TGES motif which takes part in the dephosphorylation step. By comparing several structural "snapshots" of SERCA that represent major conformations adopted during the pump cycle, it was possible to demonstrate the general mechanism how the processes at the P domain and the cation binding sites are coupled in P-type ATPases (Olesen et al., 2007). Pronounced conformational changes, especially of the A domain, are translated to the transmembrane region and the loop region. There are good indications that this leads to the alternate opening and closing of one (probably two) access pathway(s) to the binding sites.

The cation binding sites of the sodium pump were first predicted based on two atomic models of SERCA. It was possible to identify the binding sites of the Na^+,K^+-ATPase situated in the transmembrane region (Ogawa & Toyoshima, 2002). Two binding sites for K^+ and three for Na^+ were found, two of the latter seem to be alternatively occupied by Na^+ and K^+. Recently, the location of these two binding sites with occluded K^+/Rb^+ could be confirmed (Morth et al., 2007). Experimental support for the third binding site for Na^+ was also provided (Li et al., 2005). If the supposed overlap of the Na^+ and K^+ coordinating residues could be confirmed structurally, this would strongly support the idea of consecutive ion transport through the same, gated occlusion cavity. This concept is commonly called the "alternating access model" (see below). Homology modelling of Ogawa and Toyoshima proposed a strong involvement and large movements of the transmembrane helices TM4, TM5 and TM6 together with the contribution of TM8

and TM9 in cation transport which has recently received further affirmation stemming from new structural data on SERCA (Olesen et al., 2007). In addition, the Na^+,K^+-ATPase crystal structure reveals that TM1 exhibits a ~ 90° kink at the point of contact with TM3 which might provide a pivot point for TM1 movement related to ion binding (Morth et al., 2007). Several of these features have been alluded to previously in the numerous mutagenesis studies on the transmembrane region of the sodium pump.

Another interesting structural feature of the sodium pump is the location of the C-terminus (TM10), which features three consecutive arginines (Arg 1003-1005) at the intracellular membrane surface. In analogy to the voltage sensors of voltage dependent ion channels, these positively charged residues are proposed to be at least in part responsible for the sensitivity of the Na^+,K^+-ATPase to the membrane potential (Morth et al., 2007). Furthermore, close to the third putative Na^+ binding site direct contacts can be observed between tyrosines located in a kink of TM10 and lysine and arginine residues in TM5 and the TM8-TM9 loop. Depending on the membrane potential, a pull or push at the voltage sensor region could therefore be translated to the third electrogenic Na^+ binding site and affect its affinity.
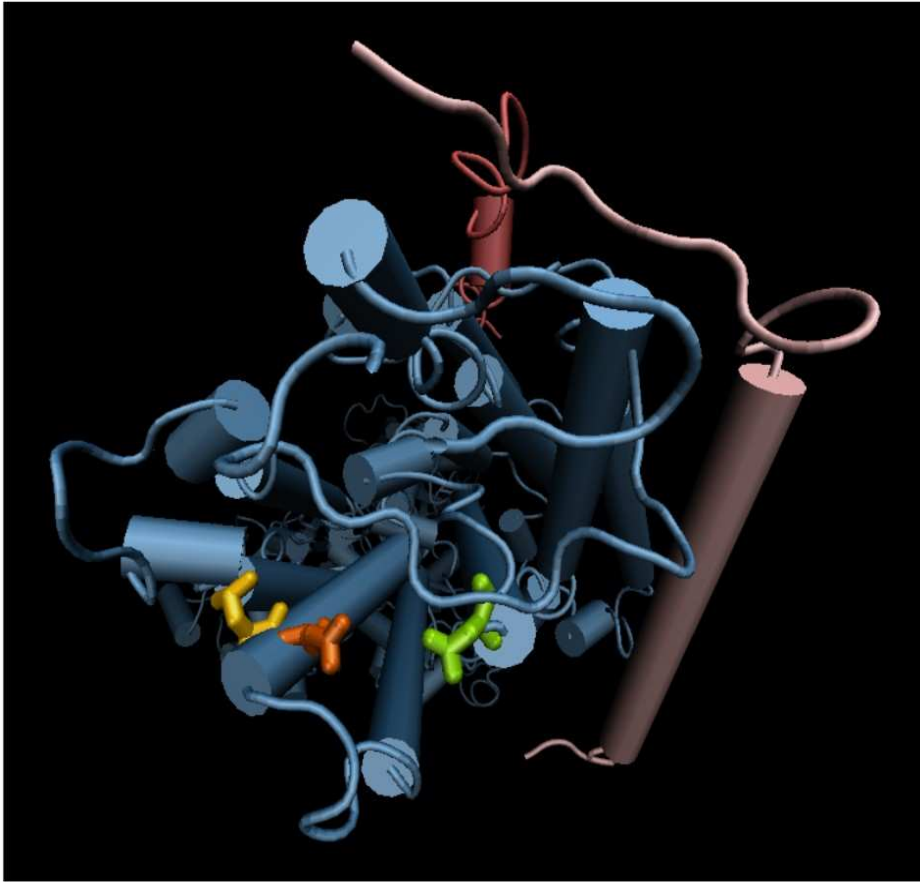
Fig. 1.2: Extracellular loop region of the Na$^+$,K$^+$-ATPase αβγ heterotrimer (blue, wheat, red). The amino acids L311, E312 and N790 that were replaced with cysteines in the study at hand are indicated in yellow, orange and green, respectively. Image created using VMD (Humphrey et al., 1996) based on structural data by Morth et al., 2007.

The architecture of the extracellular loop region of the Na$^+$,K$^+$-ATPase (shown in Fig. 1.2) was for a long time largely unknown. It is the site of action of cardiac glycosides like ouabain and digoxin that arrest the pump in the E$_2$(P) conformation. A structural model locates the binding site for cardiac glycosides in a shallow groove between TM1-TM2, TM5-TM6 and TM9-TM10 (Keenan et al., 2005). In addition, the loop region is of importance due to its involvement in ion access and egress to and from the binding sites. An egress site for Ca^{2+} in the E$_2$ form of SERCA was proposed between TM5 and TM6 (Toyoshima & Mizutani, 2004). Due to the high structural homology, the location of the binding sites and the egress site was assumed to be very similar in the Na$^+$,K$^+$-ATPase. A homology model for the sodium pump placed the TM5-TM6 loop deeply inside a crevice created by the first, second and fourth extracellular loops and therefore close to the

putative egress site (Horisberger et al., 2004). Cystein scanning mutagenesis experiments and MTSET accessibility studies on the TM3-TM4 loop of the Na^+,K^+-ATPase concluded that this loop is involved in granting access to the binding sites and therefore must be linked to the gating mechanism, but does not constitute the occlusion gate itself (Capendeguy et al., 2006). Several investigations show, that the extracellular loop region is not static during the conformational transitions of the pump-cycle. For example, the third extracellular loop between TM5 and TM6 was predicted to be dislocated during the pump cycle (Lutsenko et al., 1995). It is connected to the exterior end of the piston-like TM5 helix which links the transmembrane ion binding region to the cytoplasmic site of ATP binding and protein-phosphorylation. TM5 was therefore assumed to be involved in the energetic coupling between the two sites and, using voltage clamp fluorometry, it could show that rearrangements take place in this loop region during the conformational change of the pump (Geibel et al., 2003). Lately, the global extent of the structural reorganizations during the pump cycle of SERCA was demonstrated (Olesen et al., 2007). Due to the high structural homology of the Na^+,K^+-ATPase and SERCA the same extensive movement of extracellular -, transmembrane - and intracellular regions can be expected.

The β-subunit: The β-subunit is a type II transmembrane protein with a large, glycosylated extracellular domain (see Fig. 1.1 above). So far three different isoforms are known and their assigned functions range from governing the translation, stability and membrane insertion of the α-subunit to the modulation of cation affinities of the pump (Barwe et al., 2007; Jorgensen et al., 2003). Due to the recently resolved crystal structure of the pig renal Na^+,K^+-ATPase αβγ heterotrimer, the transmembrane helix of the β subunit can now be placed in direct contact with TM7 and TM10 at an angle of approximately 45° (Morth et al., 2007). The same study shows that the extracellular loop regions between TM5-TM6 and TM7-TM8 seem to be completely covered by the β subunit, which might account for its important role in K^+ occlusion.

FXYD proteins: In mammals, the FXYD protein family is comprised of seven members (FXYD 1-7) of which FXYD2, the γ-subunit, is probably the most commonly known (Geering, 2005). As their name implies, these proteins exhibit a common FXYD motif as well as two conserved glycine residues and a serine residue and can be considered type I membrane proteins with an extracytoplasmatic N-terminus. Their function is to modulate

pump properties like the apparent affinity for extracellular K^+ or intracellular Na^+ in a tissue-specific way (Geering, 2005). Recently, evidence was provided that the γ-subunit is located adjacent to the TM2-TM6-TM9 pocket of the α-subunit and further information on its involvement in the modulation of the apparent K^+ affinity was given (Dempski et al., 2008). In agreement with these findings, the new structural information that Morth and coworkers recently provided places the γ-subunit close to the outside of TM9 of the α-subunit and proposes an extracellular contact region with the β-subunit (see Fig. 1.1). This contact might allow the γ-subunit to modify cation affinities through the β-subunit.

1.1.2 Reaction cycle of the Na^+,K^+-ATPase

The Albers-Post scheme

The pump cycle of the Na^+,K^+-ATPase is generally illustrated by the Albers-Post scheme (Albers, 1967; Post et al., 1972) (Post et al., 1972) which describes the shuttling of the ion pump between the two main conformational states E_1 and E_2. The main features of this reaction cycle can be summarized as follows (Apell, 2004): Ion transport follows a ping-pong mechanism, which means that three Na^+ and two K^+ cross the membrane sequentially and in opposite directions. The reaction steps are: ion binding, ion occlusion (paralleled by phosphorylation or dephosphorylation of the enzyme), conformational transition, deocclusion and release of the ions. Furthermore, this transport is electrogenic, since a net charge is moved across the membrane.

The "alternating-access" mechanism

The best working model at the moment to explain the function of the Na^+,K^+-ATPase is the "alternating-access" model (Horisberger, 2004; Pavlov & Sokolov, 2000). There is increasing structural evidence to support this mechanism stemming from several crystal structures of the homologous P-type ATPase SERCA (Olesen et al., 2007). This model "expands" the Albers-Post cycle by an internal and an external gate, which sequentially opens to allow access to the ion binding sites of the Na^+,K^+-ATPase. The transition through the occluded state after ion binding with both gates closed leads to either the $E_1/E_1(P)$ or $E_2/E_2(P)$ conformation.

The reaction cycle of the Na^+,K^+-ATPase can be explained by the following scheme which includes the "alternating-access" mechanism (Fig. 1.3; taken from Horisberger 2004): In step 1, the sodium pump in its E_1 state with ATP bound to the N domain allows for the

access of 3 Na^+ ions to the ion binding sites through its open inner gate. The binding causes a conformational change which leads to phosphorylation at the P domain forming $E_1(P)$ (step 2). This in turn leads to a large conformational rearrangement of the first transmembrane segment which causes the closing of the inner gate accompanied by the release of ADP (step 3). The high energy $E_1(P)$ state quickly changes into to the lower energy $E_2(P)$ state and the outer gate opens (step 4) and the 3 Na^+ ions are consecutively released at the extracellular side (step 5). Two K^+ ions access the cation binding sites forming E_2K (step 6), dephosphorylation occurs and the extracellular gate closes (step 7). The N domain again becomes accessible to ATP and ATP binding promotes the E_2K to E_1K transition (step 8), the opening of the inner gate (step 9) and the release of K^+ at the cytoplasmic side (step 10) to complete the cycle.
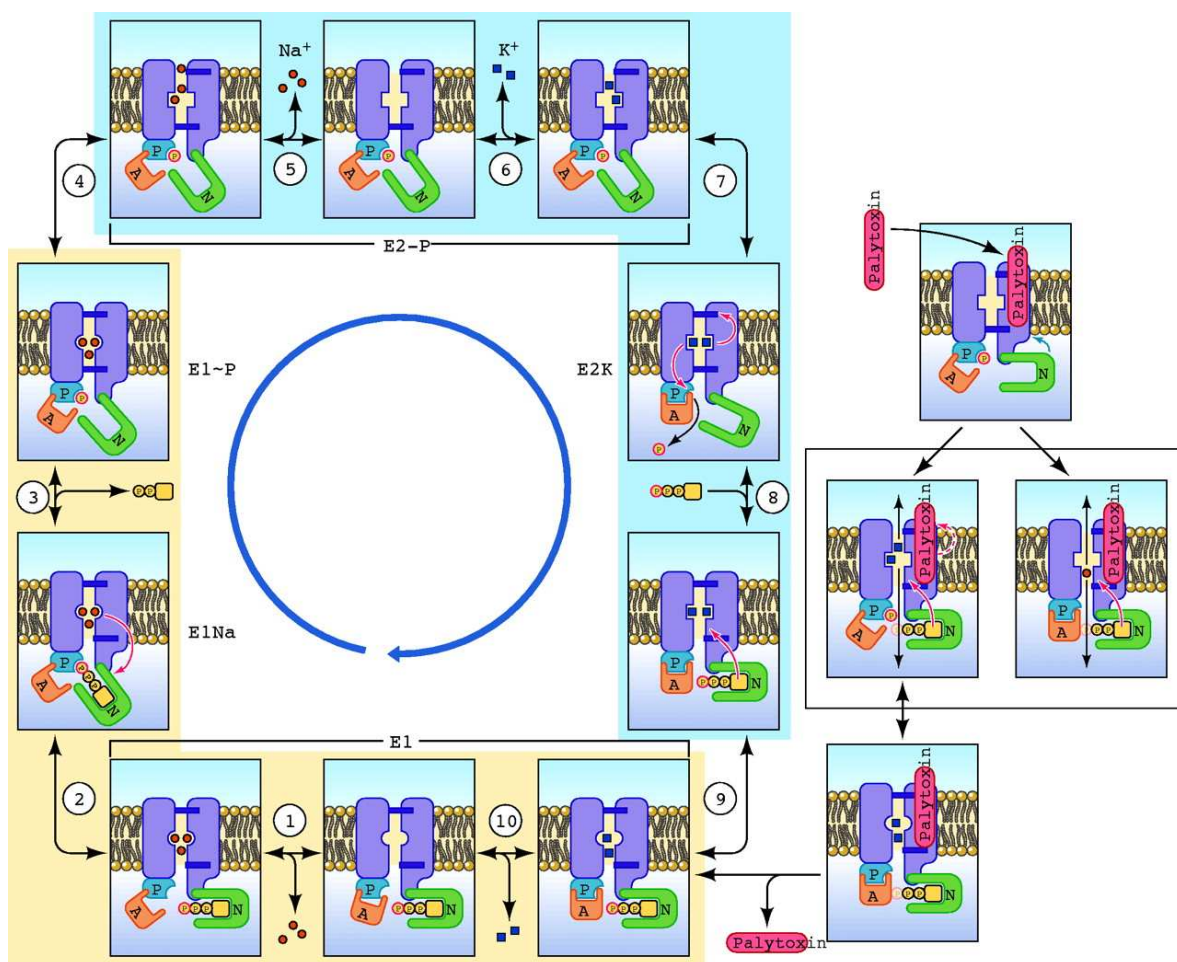

Fig. 1.3: Reaction cycle of the Na⁺,K⁺-ATPase according to the Albers-Post scheme. Integrated is the "alternating access model" (Pavlov & Sokolov, 2000) which features two gates that regulate access to the ion binding sites. The right side shows the hypothetical mechanism for the effect of palytoxin (Reyes & Gadsby, 2006), taken from Horisberger 2004.

Palytoxin

The gated channel model of the Na^+,K^+-ATPase is supported by the investigations of the sodium pump with the marine toxin palytoxin (Reyes & Gadsby, 2006). The mode of action of palytoxin seems to interfere with the coupling of the two gates. As a consequence, at times both gates are simultaneously open and the pump behaves like cation channel, but ions seem to follow the original transport route. In addition, the authors were able to gain structural information on the $E_2(P)$ conformation of the Na^+,K^+-ATPase. They produced evidence for a wide vestibule on the outside of the pump which narrows into a cation selective pore, which is another piece of evidence for the existence of an external access channel/ion well (see Fig. 1.3).

1.1.3 Electrogenicity and partial reactions of the Na^+,K^+-ATPase

Electrogenicity

Since the transport of 3 Na^+ ions outside versus 2 K^+ ions inside involves moving one net charge across the membrane, this transport is electrogenic. The charge movement influences the membrane potential - by charging or discharging the membrane capacitance – and, conversely, transport itself can be affected by the membrane potential (Apell, 2004). Originally, the definition of electrogenicity referred to the complete pump cycle and the steady state pump I/V relationship proved to be sigmoidal (Gadsby et al., 1989). Nevertheless, partial reactions of the cycle can be experimentally isolated and have also proven to be electrogenic (Nakao & Gadsby, 1986).

A

B
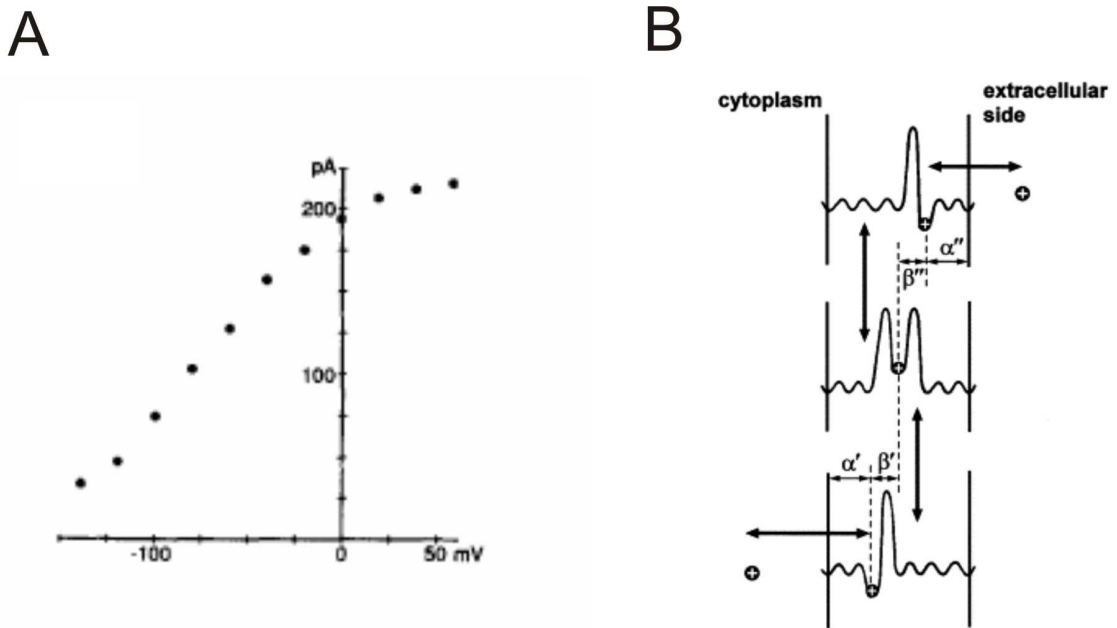
Fig. 1.4: Electrogenicity of the Na$^+$,K$^+$-ATPase. (A) Voltage dependence of the Na$^+$,K$^+$-ATPase pump currents (taken from (Nakao & Gadsby, 1986). **(B)**. Potential-energy profile of a transported ion along its pathway in states XE$_1$, (X)E$_1$-P and P-E$_2$X. The high energy barriers symbolize a virtually impenetrable structure for the ion. α′, β′, β″ and α″ represent relative dielectric distances which characterize the fraction of the membrane potential that has to be traversed by ions between two neighboring pump states. In the occluded state, equilibration between binding site and aqueous phase is blocked on both sides. Nonzero values of the dielectric distances correspond to an electrogenic contribution. Dielectric and spatial distances are not necessarily the same (taken from Apell, 2004).

To quantify the electrogenicity of a process, the "dielectric coefficient" was introduced. It describes the fraction of the membrane dielectric traversed by the moved charge during a particular reaction step. For each ion the conservation principle

α′+β′+β″+α″=1

has to be fulfilled. In the case of the Na$^+$,K$^+$-ATPase it was shown that α′ = 0.25 (Domaszewicz & Apell, 1999), β′ = 0 (Borlinghaus et al., 1987), β″ < 0.1, and α″ = 0.65 + 0.2 + 0.2 (Wuddel & Apell, 1995), with α′ and α″ representing ion binding and release, β′ and β″ representing ion occlusion and the conformational transition (see Fig. 1.4B).

Partial reactions of the Na^+,K^+-ATPase

Certain experimental conditions make partial reactions of the pump cycle accessible:

The Na^+ branch: In the absence of external K^+ dephosphorylation of $E_2(P)$ is extremely slow. The pump is virtually restricted to the Na^+ translocating branch of the cycle and can only shuttle between $E_1(P)$ and $E_2(P)$. Due to the high electrogenicity of this partial reaction, voltage jump-induced, ouabain-sensitive transient currents can be observed that decay exponentially (Nakao & Gadsby, 1986). The voltage dependence of the translocated charge during the jump protocol follows a Boltzmann relationship which describes the equilibrium populations of $E_1(P)$ and $E_2(P)$. The apparent rate constants of the charge-relaxations reach a minimum at positive potentials but increase rapidly at negative potential.

The K^+ branch: Electrical investigations of the K^+ branch of the reaction cycle are problematic due to the complicated redistribution of the reaction intermediates as long as Na^+ is present and due to its low electrogenicity.

The access channel hypothesis

It is improbable that the movement of the ion binding sites of the Na^+,K^+-ATPase alone can cover the considerably large distance of more than 4-5 nm through the pump (Lauger & Apell, 1988). Therefore, in agreement with previous considerations (Tanford, 1982), the existence of a channel was assumed which connects the binding sites with the aqueous phase. There are several indications that speak for the existence of an outward facing high-field access channel (Gadsby et al., 1993; Or et al., 1996). Structural evidence for the existence of such a feature has recently been found in SERCA (Olesen et al., 2007).

If the access channel is narrow and if it specifically promotes the passage of the transported ions it will act as an ion well. Due to its position in the membrane, a fraction of the potential difference between the extracellular and intracellular side of the membrane will drop across the length of this access channel. This will render the equilibrium dissociation constants of the transported ions at the binding sites voltage-dependent. Consequently, in the presence of an ion well, a change of electrical potential will have a similar effect as a change of the ion concentration on the occupancy of the ion binding sites (Gadsby et al., 1993; Rakowski et al., 1997).

1.2 The epithelial sodium channel (ENaC)

The epithelial sodium channel (ENaC) is important for the regulation of blood pressure and the overall body sodium balance. It consists of 3 subunits (α, β, γ) that likely form a heterotrimer, as the recently resolved structure of the closely related ASIC1 channel suggests (Jasti et al., 2007). For each subunit two transmembrane domains with short cytoplasmic C and N termini and a large extracellular loop are predicted (Rossier, 2003). ENaC is highly cation selective for Na^+ and highly sensitive to the channel blocker amiloride ($K_i = 0.1$ µM) which blocks the channel from the extracellular side. These two features make it possible to use ENaC to measure and manipulate the concentration of intracellular Na^+ when investigating other Na^+-dependent systems like the Na^+,K^+-ATPase (Crambert et al., 2000; Hasler et al., 1998; Horisberger & Kharoubi-Hess, 2002).

1.3 Fluorescence methods to resolve structure/function relations of the Na^+,K^+-ATPase

Different fluorescence methods have been applied to the Na^+,K^+-ATPase e.g. tryptophan fluorescence measurements (Karlish & Yates, 1978) measurements with 5-iodoacetamidofluorescin (5-IAF) (Sturmer et al., 1989) and RH421 (Buhler et al., 1991). The introduction of the Voltage Clamp Fluorometry (VCF) technique (Cha & Bezanilla, 1997; Mannuzzu et al., 1996) provided the means to monitor conformational changes at a specific location of an enzyme at various membrane potentials and ion conditions. For this purpose, site specific fluorescence labelling is achieved by selectively mutating an amino acid at a putative reporter positions into a cystein and covalently binding a sulfhydryl reactive fluorescence dye (Tetramethylrhodamine-6-maleimide, (TMRM)) to it. TMRM reports conformational changes in its environment due to local changes in hydrophobicity.

Previously the equivalence of the Q–V curve and the ΔF-V curve in VCF experiments with the N790C-TMRM reporter construct was demonstrated (Geibel et al., 2003). In combination with kinetic data, this lead to the conclusion that, under Na^+/Na^+ exchange conditions, the fluorescence signals report the position of the $E_1(P)$/$E_2(P)$ equilibrium. Briefly explained, the charge translocation is directly correlated to the main electrogenic step in the transport cycle, which is the release or reuptake of Na^+ on the extracellular side of the pump (Nakao & Gadsby, 1986). This electrogenic step is voltage-dependent and the application of depolarising or hyperpolarising potentials influences the position of the

$E_1(P)/E_2(P)$ equilibrium up to maximum accumulation of the enzyme in the corresponding state. Changes in fluorescence intensity recorded in parallel document the structural rearrangement during the conformational transition and likewise report the accumulation of either $E_1(P)$ or $E_2(P)$. Combined with the observation of similarly voltage-dependent kinetics of the charge translocation and fluorescence relaxations it was concluded, that the observed fluorescence-level represents an absolute measure of the concentrations of $E_1(P)$ and $E_2(P)$. VCF can be applied to gain a wealth of information about the reaction cycle of the sodium pump (Zifarelli, 2005; (Dempski et al., 2005) (Dempski et al., 2005).

The aim of this study was to examine the influence of the internal Na^+ and external K^+ concentration on the conformational equilibrium of the Na^+,K^+-ATPase and to gain information on the affected partial reactions of the pump cycle. Several partial reactions exhibit low electrogenicity and are therefore hard to study with purely electrical means. Hence, Voltage Clamp Fluorometry (VCF), which provides analogous information about the conformational equilibrium, was used to monitor the conformational changes that parallel these steps of the Na^+,K^+-ATPase reaction cycle.

2. Materials and Methods

2.1 Preparative work

2.1.1 Chemicals and solutions

Several solutions were used for the preparation and execution of the measurements in this study.

Preparative solutions	
Ori solution :	90 mM NaCl, 2 mM KCl, 2 mM $CaCl_2$, 5 mM MOPS, 100 µg/l gentamycin
Na^+-loading solution (SL):	110 mM NaCl, 2.5 mM NaCitrate, 10 mM MOPS/TRIS pH 7.4
Post-loading solution (PL):	10 mM NaCl, 1 mM $CaCl_2$, 5 mM $BaCl_2$, 5 mM $NiCl_2$, 5 mM MOPS/Tris pH 7.4
Na^+_i depletion solution (SD):	70 mM NMGCl, 40 mM KCl, 2 mM $CaCl_2$, 1 mM $MGCl_2$, 5 mM Hepes pH 7.4
TMRM-labelling solution:	Either PL or SD solution containing 5 µM TMRM
Amiloride:	100 µM to block ENaC where necessary
Measuring solutions	
Na^+-measuring solution (SMS):	100 mM NaCl, 5 mM $BaCl_2$, 5 mM $NiCl_2$, 5 mM Hepes pH 7.4, 10 µM or 10 mM ouabain.
K^+- containing measuring solutions (PMS):	similar to SMS, but different amounts of K^+ substitute Na^+ on an equimolar basis to sustain molarity.
K^+- containing NMG^+- measuring solutions (PNMS):	similar to PMS, but Na^+ is replaced by NMG^+.
Amiloride:	100 µM to block ENaC where necessary

The purpose of important solution ingredients

Na^+: The presence of Na^+_o and absence of K^+_o restricts the pump to the voltage-sensitive Na^+/Na^+ exchange mode.

K^+: A concentration of 10 mM K^+_o in the external solution is usually enough to evoke a maximal stationary Na^+,K^+-ATPase current.

NMG^+: NMG^+ is widely used as a non-transported Na^+ substitute.

Ba^{2+}: The presence of 5 mM Ba^{2+} blocks the endogenous K^+ channels of the oocyte.

Ni^{2+}: A concentration of 5 mM Ni^{2+} blocks the endogenous Na^+/Ca^{2+} exchanger of the cell and enhances the TMRM fluorescence signal (Zifarelli, 2005).

Ouabain: Ouabain prohibits stationary as well as transient currents by locking the pump in the $E_2(P)$ conformation. In this study, mutants of the Na^+,K^+-ATPase with an increased

ouabain resistance were use (described below). In such mutants, the effect of ouabain is reversible after several minutes of perfusion with ouabain-free solution.

Amiloride: 100 µM amiloride are sufficient to effectively block the epithelial sodium channel (ENaC). ENaC was in some experiments coexpressed with the Na^+,K^+-ATPase to manipulate the internal Na^+ concentration.

Tetramethylrhodamine-6-maleimide (TMRM): A cysteine-coupled fluorescent dye sensitive to hydrophobicity changes in its environment (Cha & Bezanilla, 1997).

2.1.2 Molecular biology-cRNA preparation

Na^+,K^+-ATPase

The sheep Na^+,K^+-ATPase α_1-subunit cDNA containing no exposed cysteines (carrying mutations C911S and C964A) and the rat β_1-subunit were subcloned into the pTLN-vector. For selective inhibition of the endogenous oocyte Na^+,K^+-ATPase by 10 µM ouabain, mutations Q111R and N122D were introduced into the sheep Na^+,K^+-ATPase α_1-subunit. These two mutations confer an increased ouabain-resistance to the sheep Na^+,K^+-ATPase, so that complete inhibition of the pump-currents is only achieved by 10mM oubain (as in (Jewell & Lingrel, 1991). Into this background, single cysteine mutations in the TM3-TM4 loop (L311C, E312C) and TM5-TM6 loop (N790C) were introduced by PCR and verified by sequencing.

ENaC

The rat ENaC α, β, γ subunits were linearised using Bgl II (α,β) and Pvu (γ) II**.** cRNAs were prepared by using the SP6 mMessage mMachine kit (Ambion, Austin, TX). ENaC α, β, γ subunits were a kind gift of Professor G. Nagel, Julius-von-Sachs-Institute, Würzburg.

2.1.3 Heterologous expression in *Xenopus leavis* oocytes

Oocyte preparation

Partial ovarectomy of MS222-anesthetized oocyte-positive *Xenopus leavis* females yielded, after collagenase treatment (2 mg/ml in ORI-solution for 2-4 hours), stage V/VI oocytes ready for the injection of cRNA.

cRNA injection and storage of oocytes

Na^+,K^+-ATPase expression: Each oocyte was injected with 56 nl of a stock solution containing 25 ng and 2.5 ng cRNA of the Na^+,K^+-ATPase α- and β-subunit, respectively (both cRNAs were prepared by using the SP6 mMessage mMachine kit Ambion, Austin, TX).

Na^+,K^+-ATPase/ENaC coexpression: A second stock solution containing 20 ng cRNA of the ENaC α, β and γ subunit, respectively, was prepared by using the SP6 mMessage mMachine kit Ambion, Austin, TX. Each oocyte was injected with 56 nl of a 2:1 mixture of the cRNA stock solutions (see above) of the Na^+,K^+-ATPase and ENaC.

Storage of oocytes: The oocytes were then kept at 18° C for 3-5 days in ORI-solution. In the case of ENaC expression the ORI solution contained an additional 100 µM amiloride to block ENaC (see introduction). The cells were then kept at 18° C for 3-5 days in ORI-solution containing 100 µg/l gentamycin.

2.2 Experimental procedure

Two types of experiments were performed: One type of experiments under standard experimental conditions was conducted at a saturating internal Na^+ concentration and aimed at investigating the effects of changes in the external ion composition. The other type of experiments investigated the effects of the internal Na^+ concentration on the Na^+,K^+-ATPase. To make this possible, the oocytes were depleted of internal Na^+ before these experiments were started.

2.2.1 Oocyte pretreatment and fluorescence labelling

Standard conditions

Na^+_i loading: Before performing experiments under standard conditions, $[Na^+]_i$ was elevated by incubating the oocyte in SL solution (Rakowski, 1993) for around 30 - 45 minutes on the day of the experiment. Subsequently, these oocytes were kept in the PL solution for at least another 30 minutes. This was supposed to avoid any eventual side-effects of citrate present in the SL-solution (see chapter 2.1.1).

TMRM labelling: Before using these oocytes in VCF measurements, cells were incubated in PL solution containing an additional 5 µM of TMRM for five minutes at RT, in the dark.

Then, oocytes were washed in TMRM-free PL solution to reduce unspecific dye-contaminations. The cells were kept in the dark until they were measured.
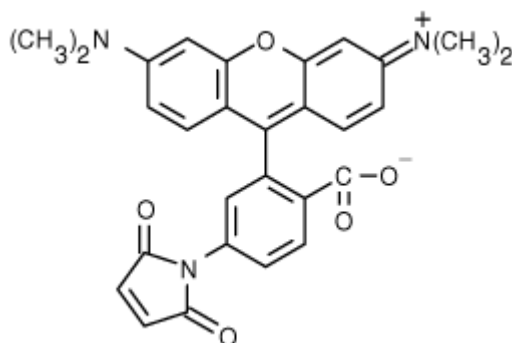

Fig. 2.1: Structure of Tetramethylrhodamine-6-maleimide (TMRM)

Na^+_i depletion conditions

Na^+_i depletion: The depletion of $[Na^+]_i$ was achieved by incubation of the cells in the SD solution, which contained NMG^+ and K^+ instead of Na^+ (see also chapter 2.1). It is assumed that this depletion of the cytosolic Na^+ can be traced back to two main transport mechanisms. Firstly, passive diffusion of Na^+ along the outward-directed Na^+-gradient through endogenous Na^+ channels (Weber, 1999). Secondly, active outward-transport of the Na^+ mediated by the Na^+,K^+-ATPase (operable in the presence of K^+_o). In agreement with a previous investigation (Horisberger & Kharoubi-Hess, 2002) the incubation time was determined to be at least 18 hours for sufficient reduction of $[Na^+]_i$ (see also chapter 2.1.1). However, oocytes showed apoptosis after subjection to incubation times longer than 48-72 hours. The survival rate of the oocytes was strongly dependent on the individual cell batch. Only cells without indication of apoptosis were chosen for subsequent experiments.

TMRM labelling: Oocytes remained in SD solution until shortly before the experiment. Then, they were labelled for 5 minutes in SD solution containing 5 µm TMRM as in standard experiments at RT and in the dark. The oocytes were immediately washed in SD solution and kept in this solution in the dark until their transfer to the measuring-chamber.

2.2.2 Two electrode voltage clamp fluorometry

The VCF set-up

A fluorescence microscope (Axioskop 2FS, Carl Zeiss MicroImaging, Inc.) with a 40x water-immersion objective (numerical aperture = 0.8) was equipped with a custom-made

oocyte perfusion-chamber. Electrical measurements were performed with a two-electrode voltage clamp amplifier CA-1B (Dagan Instruments), which was connected via an analog-digital converter Digidata 1200B (Axon instruments) to a personal computer running pClamp 9-software (Axon instruments).

Intracellular voltage recording and current electrodes were Ag/AgCl electrodes with glass-pipette tips (GB 150-8P, Science Products GmbH, Hofheim) filled with 3M KCl, with a resistance of less than 3 MΩ. Bath electrodes were low resistance agar bridges connected to Ag/AgCl electrodes in compartments containing 3 mM KCl. For fluorescence measurements, a 100 Watt tungsten lamp was used as a light-source, combined with a 535DF50 excitation filter and a 565EFLP emission filter and a 570DRLP dichroic mirror (Omega Optical). Fluorescence was detected by a PIN-022A photodiode (United Detector Technologies) and amplified by a patch clamp amplifier EPC (HEKA Electronics). Fluorescence data was stored and processed on the personal computer using the pClamp9 software. The solution exchange was accomplished with a manually operated 8-times perfusion-system (ESF Electronic, Germany) supported by a pump for rapid removal of excess fluid. All experiments were performed on the vegetal pole of *Xenopus* oocytes at 20-22° C and in the dark, whenever fluorescence was recorded.
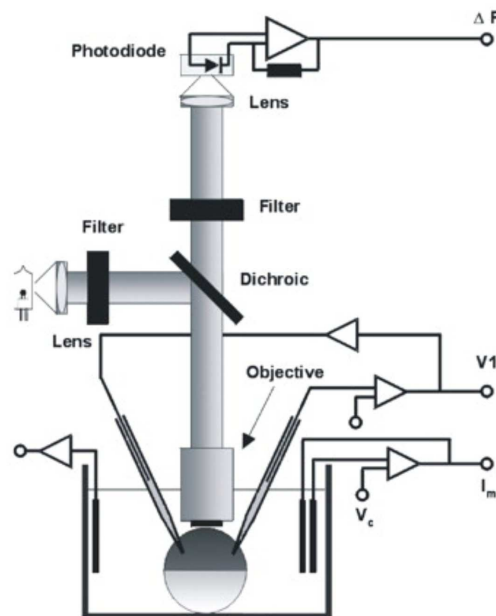

Fig. 2.2: Experimental set-up (Dempski et al., 2005).

Voltage step protocols and data acquisition

For measurements of the Na^+,K^+-ATPase, one of two "long" voltage step protocols was used. Both protocols consisted of two succeeding step-ladders which were approached from two different holding potentials (HP = -80 mV and HP = 0 mV, respectively). The first protocol followed voltage steps from +80 mV to -180 mV in fourteen 20 mV steps (600 ms long), the second protocol followed voltage steps from +100 to -200 mV in eleven 30 mV steps (330 ms long) to further extend the observed potential range for certain experiments.

For determination of the ENaC I/V curve a "short" protocol was used, which allowed only minimal inflow of Na^+_o during this amiloride-free measurement and therefore had no significant effect on the internal sodium concentration. The protocol was set to perform seven 20 mV voltage steps (650 ms long) from a holding potential of -80 mV and covering a range between +100 mV and -20 mV.

Data was always averaged from two runs. The sampling rate was 25 kHz and filtering occurred at 2 kHz, respectively.

Exchange of external Solutions

Perfusion: To examine the effects of various successively applied external ion-solutions on the different Na^+,K^+-ATPase constructs in this study, the measuring-chamber was usually perfused with the new solution for 2-3 minutes before the next measurement was started to assure a complete solution exchange. During the perfusion, the current-clamp (CC) mode was chosen to reduce the stress on the oocyte and to additionally monitor the solution exchange via the membrane potential, which reacts very sensitively to changes of the external ion-composition. A new measurement was not initiated before the membrane potential had reached a stable value. During the actual recordings, the solution-flow was stopped to avoid any negative effects of oocyte-movement or noise from the suction-mechanism.

Correction for bleaching: The unavoidable decrease of the fluorescence signal over time due to bleaching was, during longer measurements monitored by intermediate recordings in SMS and was later corrected for (see below).

Manipulation of $[Na^+]_i$

Increase of $[Na^+]_i$: In experiments in which the effect of an increase of the internal sodium concentration $[Na^+]_i$ was to be studied, the Na^+_i-depleted cell was loaded with Na^+ in a step-by-step manner. For each step, $[Na^+]_i$ was determined (see below) and the fluorescence of the Na^+,K^+-ATPase-TMRM sensor complex recorded.

The first measurement was always performed in SMS containing 100 µM amiloride using one of the long voltage step protocols mentioned above. This protocol was followed by the short voltage-step protocol in amiloride-free solution, to open ENaC for the determination of the reversal potential of Na^+ and to slightly raise $[Na^+]_i$. Alternate application of these two protocols and solutions was repeated until a $[Na^+]_i$ of more than 50-60 mM was reached.

When necessary, inflow of Na^+ through the open ENaC channel was significantly increased by applying a holding-potential (HP) of -100 mV for 1-2 minutes.

Correction for bleaching: Experimental difficulties (see below) prevented the introduction of intermediate recordings to monitor the bleaching in experiments described above. Hence, another method was chosen to avoid fluorescence intensity-loss over time. The iris-like shutter of the VCF set-up, which regulates the illuminated area of the cell, was opened slightly to compensate for intensity-loss whenever the background fluorescence had dropped more than 2-3 % of the starting value. This correction was repeated as often as necessary.

Determination of $[Na^+]_i$: The reversal potential (RP) for Na^+ was determined from the intersection of pairs of I/V-curves measured with and without amiloride (see above). The $[Na^+]_i$ of the very first fluorescence measurement could always only be estimated due to the fact, that it could not be preceded by an I/V-curve measurement with open ENaC channels, because this recording by itself would lead to a change in $[Na^+]_i$. Yet, for all other measurements the sequence of recordings allowed the calculation of $[Na^+]_i$ by knowledge of $[Na^+]_o$ (100 mM) and use of the Nernst-equation:

$$[Na^+]_i = [Na^+]_o \exp(-FV/RT)$$

where F, R, T have their usual meanings and V is the reversal potential of the amiloride sensitive current.

Experimental difficulties: The experimental procedure used did not allow to fix $[Na^+]_i$ to a desired value which made the implementation of concentration intervals necessary (see below). It was only possible to approximate the internal Na^+ concentration. This was done by switching to CC-mode during the loading-procedure and using the RP, which mainly reflects the RP of Na^+, to assess $[Na^+]_i$.

Another experimental difficulty was an often present, unspecific and variable inflow of Na^+_o into the oocyte which often prevented the performance of several consecutive experiments at low $[Na^+]_i$. This inflow seemed very much dependent on the leak tightness of the oocyte-membrane. The main reason for this Na^+ inflow could therefore be the incomplete resealing of the membrane at the sites of electrode impalement, especially when cells were of lower quality. Additionally, endogenous Na^+ channel and pumps of the oocyte-membrane not blocked by the reagents present in the utilised solutions (see above) could lead to the inflow of Na^+_o.

2.3 Data analysis

Generally, the signals analyzed were "on"-signals form a holding potential of -80 mV to a specific target-potential of the voltage step protocol. In the case of the E312C construct, the kinetics of the fluorescence changes were partly determined from a HP of 0 mV, due to the bigger changes in fluorescence intensity that jumps from this HP to the target potentials evoked. This approach is justified by the fact, that the kinetics of the voltage jump-induced relaxations are only determined by the target potential and not the HP.

Original current and fluorescence traces were analyzed in Clampfit 9. Fit parameters were exported to Origin 7 for further analysis, but determination of the apparent translocated charge, z_q, was also performed in Clampfit 9. For the finalisation of graphs Corel Draw 11 was used.

2.3.1 Stationary current measurements

Measuring procedure: Under voltage clamp conditions in PMS-solution (typically at HP = -40 mV), the presence of 10 mM external K^+ evokes a positive, pump-specific outward-current of the expressed Na^+,K^+-ATPase, which is practically completely inhibited by addition of 10 mM ouabain.

Test for functionality after TMRM-modification: The difference between the inhibitable K^+-induced stationary current before and after cysteine-specific modification with TMRM was used to gauge the functionality of all the Na^+,K^+-ATPase mutants used in this study.

2.3.2 Transient current measurements

Measuring procedure and subtraction method: Using the pClamp 9 software, the oocytes in SMS were subjected to one of the two voltage-step protocols mentioned earlier, depending on the voltage-range of interest. Repetition of the same protocol in solution containing 10 mM Ouabain and subtraction of both sets of current-traces yielded transient difference currents characteristic of the voltage-dependent Na^+/Na^+ exchange mode of the pump (Nakao & Gadsby, 1986).

Fitting procedure: The transient current-traces were approximated by a monoexponential function which started after the capacitive artefact of membrane-charging (which can last several ms). The fit allowed the determination of the apparent relaxation rate (τ^{-1}), for the decay of these transient currents. Furthermore it was possible to calculate the amount of translocated charge Q from the integral of the transient current. The calculated charge, Q, exhibits a sigmoidal voltage-dependence that can be described by a Boltzmann function with an apparent valence, z_q, of 1.0, which is appropriate for a single charge translocated over the entire membrane field (see introduction).

$Q(V)=Q_{min}+(Q_{max}-Q_{min})/(1+exp(z_qF(V-V_{0.5})/RT))$

where F, R, T have their usual meanings, z_q is the apparent valence, $V_{0.5}$ is the midpoint potential and Q_{min} and Q_{max} are the saturation values of the sigmoidal distribution at extreme potentials. The midpoint potential, $V_{0.5}$, can be used as a measure for the ion affinity. In addition, z_q can be calculated, to give information about the apparent amount of charge moved through the membrane field during the observed process.

Test for functionality after TMRM-modification: The above mentioned relaxation rate coefficients of the transient currents before and after the modification with TMRM were compared for each mutant to detect a possible slow-down of the Na^+/Na^+ exchange reaction due to the covalent binding of the fluorophore.

2.3.4 Fluorescence measurements

Analysis of the transient fluorescence changes

Fluorescence traces obtained from the Na^+,K^+-ATPase-TMRM sensor complexes via the voltage clamp fluorometry (VCF) technique were generally approximated by a single exponential function in a good manner (Dempski et al., 2005; Geibel et al., 2003). In the light of the literature the approximated fluorescence signal was correlated with the conformational change of the protein (Geibel et al., 2003).

Multiple components: However, in some experiments the main fluorescence component was superimposed by a very fast ($\tau < 2$ ms) and/or a very slow fluorescence component ($\tau > 200$ ms) in respect to the main component. It has to be mentioned that these additional fluorescence components revealed only small amplitudes.

The fast fluorescence component revealed a time constant similar to the relaxation constant of the capacitance artefact and therefore is maybe originated in the artefact. However, a similar fast component was observed in VCF experiments with the *Shaker* potassium channel (Cha & Bezanilla, 1997). The group explained the observed fast fluorescence signal with a high- and low-fluorescence intermediate state, respectively. Discrimination between these two possible explanations was not possible and the fast component was neglected in the subsequent analysis.

The slow fluorescence component, in turn, revealed a time constant, which was identified to be similar to the simultaneously occurring leak currents (data not shown). Therefore, it seems to be self-evident, that the slow component is due to an insufficient voltage clamp of the oocyte. It has to be mentioned, that this effect seems to be exclusively observable for the mutant L311C (similar findings for the H^+,K^+-ATPase S806C, private communication D. Zimmermann). A possible explanation is that the fluorophor (TMRM) is, at this position, very sensitive to the changes in membrane voltage and, subsequently, to the occurrence of an inhomogeneous voltage clamp of the oocyte.

For the sake of simplicity, the fluorescence component revealing conformational changes of the L311C pump was extracted by results of a biexponential approximation of the data starting with a 2 ms delay after the applied voltage jump and only the fast component of this fit was analyzed further.

It should be mentioned, that recent structural data suggest, that in P-type ATPases the 2nd extracellular loop moves simultaneously and relative to the 1st and 3rd loop during

certain sections of the pump cycle (Olesen et al., 2007). A biphasic time course of the fluorescence relaxation is therefore generally imaginable.

Correction for bleaching: To correct for fluorophore bleaching, each intermediate measurement in SMS in a series of measurements (see above) was fit by a Boltzmann function. The resulting total amplitude of each Boltzmann fit was then compared to the amplitude of the 1st, unbleached fit in the series. By division, a correction factor for the amplitude decrease caused by bleaching was determined for each intermediate measurement in SMS. This factor was then applied to correct for the amplitude-bleaching of the following measurement performed under the experimental conditions of interest.

Normalization: As was mentioned above, voltage-jumps induce fluorescence changes in several TMRM-labelled Na^+,K^+-ATPase mutants (Dempski et al., 2005; Geibel et al., 2003; Zifarelli, 2005). The saturation values of these fluorescence changes follow a Boltzmann function when plotted against the membrane potential (ΔF-V curve). The parameters of the Boltzmann function (total amplitude A, midpoint potential, $V_{0.5}$, and apparent translocated charge, z_q) give evidence about the $E_1(P)/E_2(P)$ equilibrium, the ion affinity and the electrogenicity of the process. Yet, the introduction of certain mutations or the change of specific external conditions (Geibel et al., 2003) or internal conditions (e.g. $[Na^+]_i$, ATP, ADP, etc.) can substantially change these parameters.

Therefore, for the best comparison of fluorescence signals of various mutants and under different conditions, all Boltzmann fits to the fluorescence data were normalized to the Boltzmann fit belonging to the measurement in SMS with the biggest change in fluorescence, ΔF, (i.e. measured under saturating $[Na^+]_i$ conditions and least affected by bleaching). Under standard conditions, this was usually the 1st measurement in SMS in a series of measurements. When the increase of $[Na^+]_i$ was monitored, the measurement showing the biggest ΔF after $[Na^+]_i$ reached saturation was chosen.

If possible, normalized fits were aligned along the y-axes according to their position determined by the background fluorescence that was measured during the original fluorescence recordings. In case this was not possible, fits were aligned so that saturating fluorescence values upon hyperpolarisation coincided with E_1 or $E_1(P)$, respectively.

Concentration-intervals: Due to the experimental constraints mentioned above, $[Na^+]_i$ could not be fixed to a desired value and measurements from different oocytes could not be directly combined and compared at a certain concentrations. Therefore, to be able to match several cells of each Na^+,K^+-ATPase mutant, three $[Na^+]_i$-intervals were designated after

preliminary experiments which had determined the approximate K_m-value for $[Na^+]_i$ (~ 10 mM). One interval represents low $[Na^+]_i$ (up to 10 mM), one interval medium $[Na^+]_i$ (10-20 mM) and one interval high/saturating $[Na^+]_i$ (above 20 mM).

For each mutant, the means and standard deviations of 3 cells were determined in each interval. To establish a more precise concentration dependence for $V_{0.5}$ and z_q the intervals were defined by the actually measured minimal and maximal concentration values. *Measurements at very low $[Na^+]_i$:* In two experiments, $[Na^+]_i$ was extremely low, indicated by the observation, that the first fluorescence-measurement yielded no, or almost no noticeable fluorescence changes upon application of the voltage step protocol. This circumstance made it possible to monitor the influence of minute increases of $[Na^+]_i$ on the voltage jump-induced fluorescence changes by simply relying on the unspecific inflow of Na^+_o over time, instead of using the usual voltage step procedure (see above).

As a draw-back of this method, the determination of $[Na^+]_i$ using reversal potential measurements was not possible because the employed step protocol would have raised the internal sodium concentration by a too large amount. Yet, the analysis of previous data enabled us to describe the relationship between $V_{0.5}$ and $[Na^+]_i$ that seems to become prominent at $[Na^+]_i$ below 10 mM. Within limits, this relationship can be qualified reasonably well by a monoexponential function

$$y = A_1 exp(-x/t_1) + y_0$$

with $y_0 = -152$, $A_1 = 300$ and $t_1 = 0.002$ to approximate the unknown $[Na^+]_i$. Here, y_0 is the saturation value of $V_{0.5}$ at saturating $[Na^+]_i$, A_1 the starting value of $V_{0.5}$ at $[Na^+]_i = 0$ mM, t_1 the constant describing the relaxation and x representing the unknown $[Na^+]_i$.

3. Results – Investigation of the mutant N790C

In order to gain further understanding of the K^+ branch of the sodium pump, previous experiments featuring the N790C-TMRM reporter complex (Geibel, 2003; Geibel et al., 2003) were extended by investigations under Na^+ free conditions. Moreover, it was of interest to see if this external reporter position could be used to monitor the putative effects that changing the internal Na^+ concentration should have on the Na^+ branch of the reaction cycle (Holmgren & Rakowski, 2006).

3.1 Characterization of N790C

Residue N790 is located in the third extracellular loop of the sodium pump connecting the transmembrane helices TM5 and TM6. In previous studies, voltage-induced charge movements of the Na^+,K^+-ATPase N790C construct and the corresponding TMRM-mediated fluorescence signals of the N790C-TMRM sensor complex have been studied in TEVC experiments on *Xenopus* oocytes (Geibel et al., 2003). It was found that both charge translocation and changes in fluorescence intensity, could be traced back to the $E_1(P)/E_2(P)$ transition of the pump and the corresponding movement of the TM5 helix, respectively.

3.1.1 General Characteristics of N790C described in the literature

Charge translocation and changes in fluorescence intensity

In Fig. 3.1A the data of five TEVC fluorometry experiments performed on the sensor complex TMRM-N790C under Na^+/Na^+ exchange conditions are shown (Geibel et al., 2003). The fluorescence saturation values ΔF and the translocated charge Q in response to changes in the membrane potential were normalized and approximated by Boltzmann functions. It is known that hyperpolarisation shifts the conformational equilibrium towards $E_1(P)$ and depolarisation towards $E_2(P)$ (Nakao & Gadsby, 1986; Rakowski, 1993). Since both the ΔF-V and the Q-V show the same voltage dependence it was determined, that the TMRM-mediated fluorescence changes can be used to directly gauge the $E_1(P)/E_2(P)$ ratio.
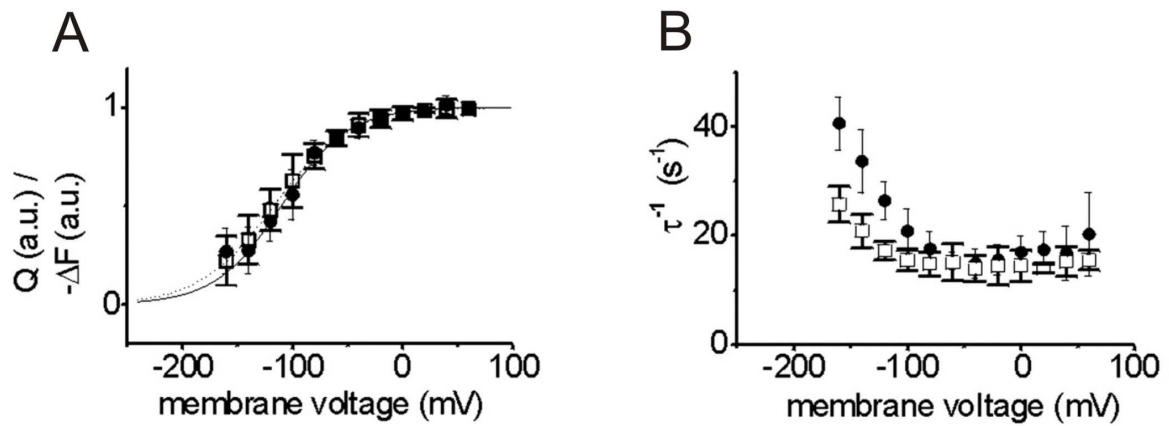
Fig. 3.1: Na$^+$,K$^+$-ATPase Mutant N790C. Electrical and fluorometric characterization. (A) Voltage dependence of the fluorescence saturation values ($\forall$) and the translocated charge (.). Normalized VCF data. Fits of the Boltzmann functions are superimposed, yielding the following parameters: $V_{0.5}$ (fluorescence) = -117 ± 1mV, $V_{0.5}$ (charge) = -110 ± 9mV, z_q (fluorescence) = 0.8 ± 0.2, z_q (charge) = 0.9 ± 0.1. **(B)** Rate constants (reciprocals of time constants) of fluorescence changes ($\forall$) and transient currents (.). All data are means ± SE of five cells (Geibel et al., 2003).

Kinetics

In Fig. 3.1B the apparent rate constants, τ^{-1}, associated with the particular voltage-step induced charge movements and fluorescence changes of Fig. 3.1A are shown. As mentioned above, Geibel et al., 2003 concluded that the conformational state of the ion pump can be determined with the TMRM-mediated fluorescence. This assumption is supported by the high level of similarity of the kinetic data of both observed processes. However, the kinetics of the monitored conformational change are slightly slowed down, maybe as a result of the attached TMRM. In an independent experiment the data presented in Fig. 3.1 were confirmed and therefore subsequently used as a "starting point" of the present study.

3.1.2 Characteristics of the ENaC/N790C–system

Following the investigations of (Horisberger & Kharoubi-Hess, 2002) we chose to study the effects of low [Na$^+$]$_i$ on the $E_1(P)/E_2(P)$ equilibrium and the kinetics of the conformational transition of the sodium pump using the VCF suitable N790C-TMRM sensor complex in combination with an epithelial sodium channel ENaC. In order to verify the functionality and characterize this combined system, the effects of opening/closing the ENaC channel on stationary pump-currents and on TMRM-mediated fluorescence (under Na$^+$/Na$^+$ exchange conditions) were investigated. It has to be stated, that oocytes were

initially depleted of Na^+_i to monitor the concentration-increase (see section Materials and Methods).

Stationary currents

The stationary current recording of an oocyte expressing the ENaC/N790C-system in Fig. 3.2A shows the typical response of the Na^+,K^+-ATPase to a step-wise, ENaC-mediated increase of $[Na^+]_i$. Opening ENaC by removing its blocker amiloride causes an inward-directed flow of Na^+ along the Na^+ gradient, thereby increasing $[Na^+]_i$. As reported previously (Holmgren & Rakowski, 2006), suboptimal $[Na^+]_i$ are likely to interfere with the Na^+_i–binding of the pump (transition of $E_1P \rightarrow E_1P(3Na^+)$ in the Albers-Post reaction scheme). As a consequence, the K^+_o–inducible stationary current increases when $[Na^+]_i$ is raised.
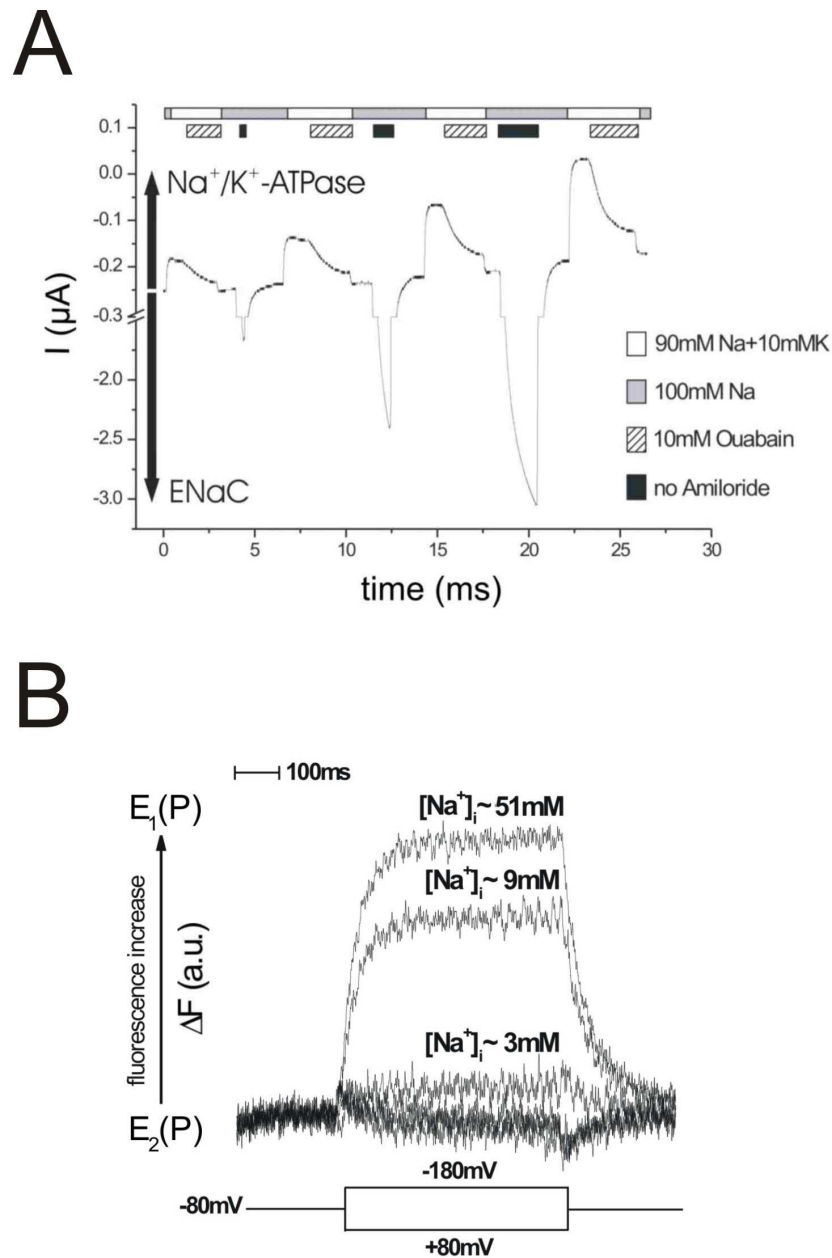
Fig. 3.2: Na$^+$,K$^+$-ATPase Mutant N790C. Manipulation of [Na$^+$]$_i$ by coexpression of ENaC. (A) Dependence of the Na$^+$,K$^+$-ATPase pump current on [Na$^+$]$_i$. Current recording of an oocyte expressing the ENaC/N790C-system. Successive removal of amiloride for a limited amount of time leads to a step-wise increase of [Na$^+$]$_i$ due to a Na^+_o inward current through ENaC. This, in turn, steadily increases the ouabain-inhibitable outward current of the Na$^+$,K$^+$-ATPase, which is induced by external application of 10 mM K$^+$. (B) Fluorescence signals of the Na$^+$,K$^+$-ATPase in Na$^+$/Na$^+$ exchange mode at three different [Na$^+$]$_i$. Hyperpolarisation from HP = -80 mV to -180 mV evokes fluoresce-signals of increasing amplitude with rising [Na$^+$]$_i$. Changes in response to depolarisation to +80 mV were negligible.

Changes in fluorescence intensity in response to voltage jumps

Fig. 3.2B displays the typical voltage-step-induced fluorescence signals of a TMRM-labelled oocyte expressing the ENaC/N790C-system under Na$^+$/Na$^+$ exchange conditions

(see section Materials and Methods) at three different concentrations of Na^+_i. Hyperpolarisation (from -80 mV to -180 mV) promotes a shift of the equilibrium from $E_2(P)$ to $E_1(P)$. Obviously, larger fluorescence-changes are induced when sub-membrane $[Na^+]_i$-levels are elevated. In contrast to this, the signals due to depolarisation to +80 mV are basically unaffected by an increase of $[Na^+]_i$.

3.2 Effect of the internal sodium concentration

To evaluate the effect of the internal Na^+ concentration on the conformational equilibrium cells were subjected to voltage steps under Na^+/Na^+ exchange conditions after each increase of $[Na^+]_i$. This enabled us to monitor the consequences of the concentration increase in an isolated part of the reaction cycle: the Na^+ branch and the associated $E_1(P)/E_2(P)$ transition.

3.2.1 Measurements at very low $[Na^+]_i$

In some experiments it was possible to achieve thorough depletion of internal Na^+ and, subsequently, minute increases of Na^+_i could be recorded. However, it should be noted that in such experiments low concentrations of internal Na^+ had to be determined by using an extrapolation-method (see Materials and Methods).

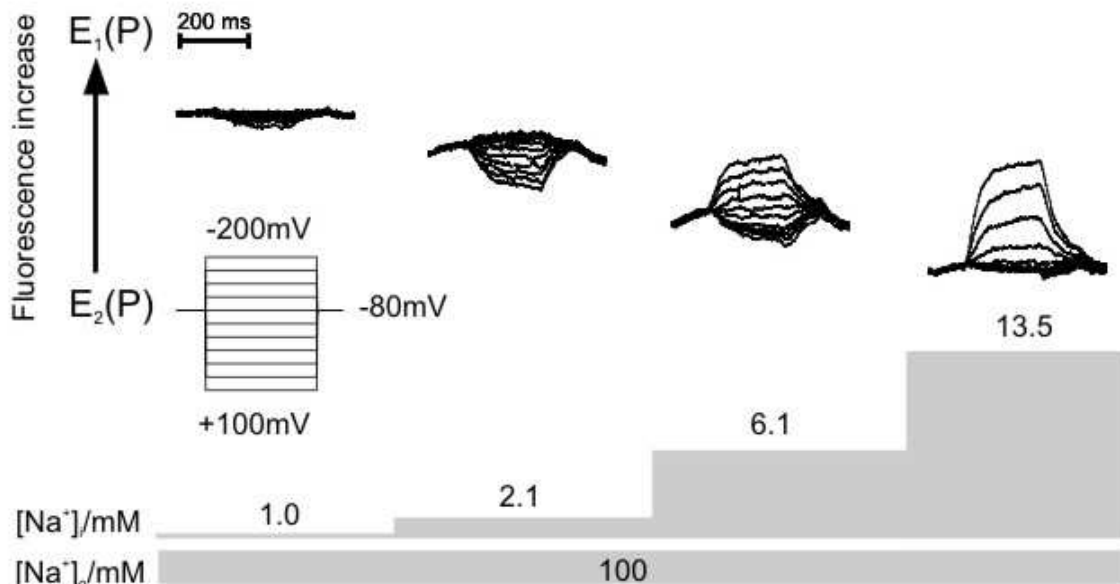**Fig. 3.3: Na+,K+-ATPase Mutant N790C. Minute increases of [Na+]i.** Voltage jump-induced fluorescence changes under Na^+/Na^+ exchange conditions from a continuous recording of a single oocyte at different $[Na^+]_i$. Effect on the $E_1(P)/E_2(P)$ equilibrium. Due to uncompensated fluorophore bleaching the decrease in fluorescence does not quantitate the shift of the conformational equilibrium.

Four consecutive recordings depict fluorescence responses following an increase of the intracellular Na^+ concentration (Figure 3.3). To isolate the Na^+ branch of the reaction cycle (Na^+/Na^+ exchange conditions) the extracellular solution contained 100 mM Na^+. At the start of the experiment, no changes in fluorescence were observable. After increasing the Na^+_i-concentration ($[Na^+]_i = 1.0$ mM) changes in fluorescence intensity can be evoked, but only as the result of depolarising potentials steps. This observation is usually associated with a conformational equilibrium that is primarily located in $E_1(P)$ (Geibel et al., 2003). Raising $[Na^+]_i$ to 2.1 mM increases the size of the changes in fluorescence intensity upon depolarisation and allows for fluorescence changes in response to hyperpolarising voltage steps. Continued increase of the internal Na^+ concentration ($[Na^+]_i = 6.6$ mM) boosts the magnitude of the evocable fluorescence responses resulting from hyperpolarisation, whereas signals upon depolarisation become smaller. At $[Na^+]_i = 13.5$ mM the fluorescence responses are basically identical to those acquired in previous experiments performed at a saturating concentration of internal Na^+. Under this condition most pump molecules reside in the $E_2(P)$ conformation but can be shifted to $E_1(P)$ by hyperpolarisation (Geibel et al., 2003). The decrease in background fluorescence suggests a shift of the conformational equilibrium towards $E_2(P)$. However, this shift can not be quantitated since it is overlayed by uncompensated fluorophore bleaching.

3.2.2 Measurements covering an extensive $[Na^+]_i$ -range

Changes in fluorescence intensity

In order to compare data from several cells, the concentration range was divided into three concentration intervals representing low (1 - 10 mM, black), medium (10 - 20 mM, red) and high/saturating (20 - 70 mM, green) internal Na^+ concentration (see Materials and Methods). Fig. 3.4A shows the averaged ΔF-V data of three independent VCF experiments (means $\pm$ SD) performed under Na^+/Na^+ exchange conditions. All data were approximated by Boltzmann functions and normalized to the ΔF-V curve acquired under saturating $[Na^+]_i$ conditions (green). To establish a more precise concentration dependence the intervals in Fig. 3.4B and C are defined by the actually measured minimal and maximal concentration values. Fig. 3.4D depicts the voltage dependence of the averaged apparent rate constants (means $\pm$ SD) in each concentration interval.
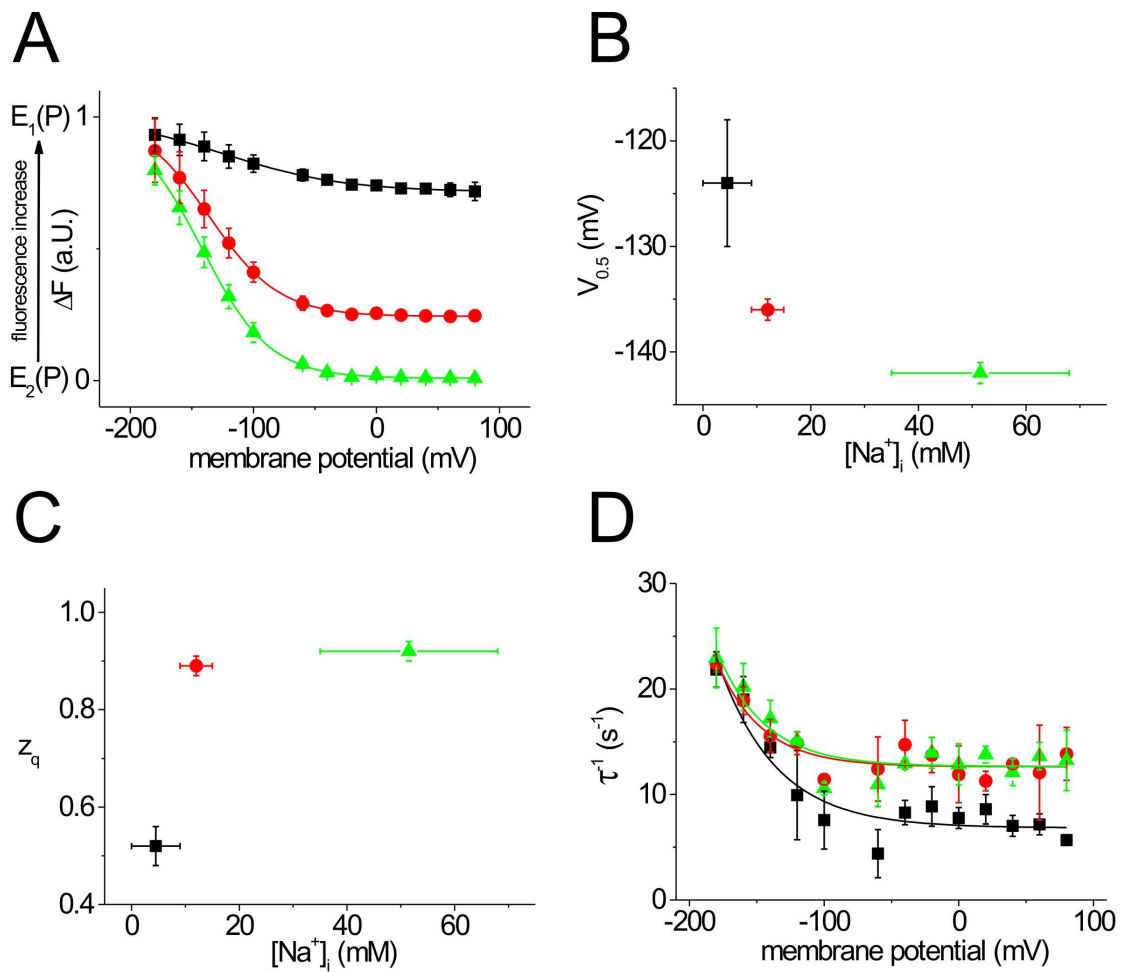
Fig. 3.4: Na$^+$,K$^+$-ATPase Mutant N790C. [Na$^+$]$_i$ concentration intervals. (A) Voltage dependence of the fluorescence saturation values organized into concentration intervals of low (!), medium (,) and saturated (7) [Na$^+$]$_i$. Data presented as means ± SD of 3 cells and the corresponding Boltzmann curves. All voltage steps were executed from HP = -80mV **(B)** Dependence of the midpoint potential V$_{0.5}$ of the Boltzmann curves on [Na$^+$]$_i$. Concentration intervals stretch from the minimal to the maximal [Na$^+$] measured for more precise localization on the x-axes. Data presented are fit parameters of Boltzmann functions and their standard errors. **(C)** Dependence of the apparent translocated charge z$_q$ on [Na$^+$]$_i$. representation as in (B). **(D)** Apparent rate constants of the original fluorescence relaxations organized into concentration intervals as in (A). Data presented as means ± SD of 3 cells and the corresponding monoexponential functions.

At the first glance, the most noticeable effect of an increase of [Na$^+$]$_i$ is an enlargement of the evoked changes in fluorescence intensity (compare the increase in total amplitude of the three different Boltzmann fits). In addition, at medium and high [Na$^+$]$_i$ large changes in fluorescence intensity are only induced by voltage steps starting from the HP = -80 mV to more hyperpolarising membrane voltages. In contrast, at low [Na$^+$]$_i$, the changes in fluorescence intensity evoked by depolarising voltage-steps are proportionally larger due to the smaller fluorescence changes at hyperpolarising potentials.

Two parameters that provide information about the monitored partial reaction of the cycle - the midpoint potential, $V_{0.5}$, and the apparent translocated charge, z_q - were obtained from the corresponding Boltzmann fits of the ΔF-V data.

Interestingly, Fig. 3.4Bshows that $V_{0.5}$, which gives information about the cation affinity of the pump (Dempski et al., 2005; Geibel et al., 2003) is shifted by ~ 18 mV towards hyperpolarising potentials upon an increase of $[Na^+]_i$ (from -124 ±6 mV to -136 ± 1 mV and -142 ± 1 mV, respectively).

Fig. 3.4C displays that z_q, the apparent translocated charge attributed to the external Na^+ release/rebinding process (Dempski et al., 2005; Geibel et al., 2003), is smaller at low $[Na^+]_i$ than at medium or high concentrations (0.52 ± 0.05, 0.89 ± 0.02 and 0.92 ± 0.02, respectively).

Kinetics

The apparent rate constants, τ^{-1}, of the particular voltage step-induced fluorescence relaxations of all three concentration-intervals (mean ± SD, n = 3) are shown in Fig. 3.4D. Irrespective of $[Na^+]_i$, a typical, voltage-dependent acceleration of the kinetics at hyperpolarising potentials is observed (Friedrich & Nagel, 1997; Geibel et al., 2003). However, compared to the kinetics at medium and high $[Na^+]_i$, which exhibit no concentration-dependent effect, low $[Na^+]_i$ leads to a slow-down of the fluorescence relaxations. This seems to be restricted mostly to depolarising potentials.

3.3 Effect of external potassium

In the presence of extracellular K^+, dephosphorylation of the pump is accelerated and the K^+ branch is opened, thereby allowing for turnover of the pump. Voltage dependent Na^+ rebinding can occur that slows down forward pump turnover (De Weer et al., 2001). However, under these conditions transient currents can no longer be observed due to kinetic reasons (Bahinski et al., 1988; Geibel et al., 2003). Yet, by application of the VCF method, information on the monitored conformational change and the $E_1(P)/E_2(P)$ equilibrium can still be obtained (Geibel et al., 2003).

3.3.1 Substitution of external sodium

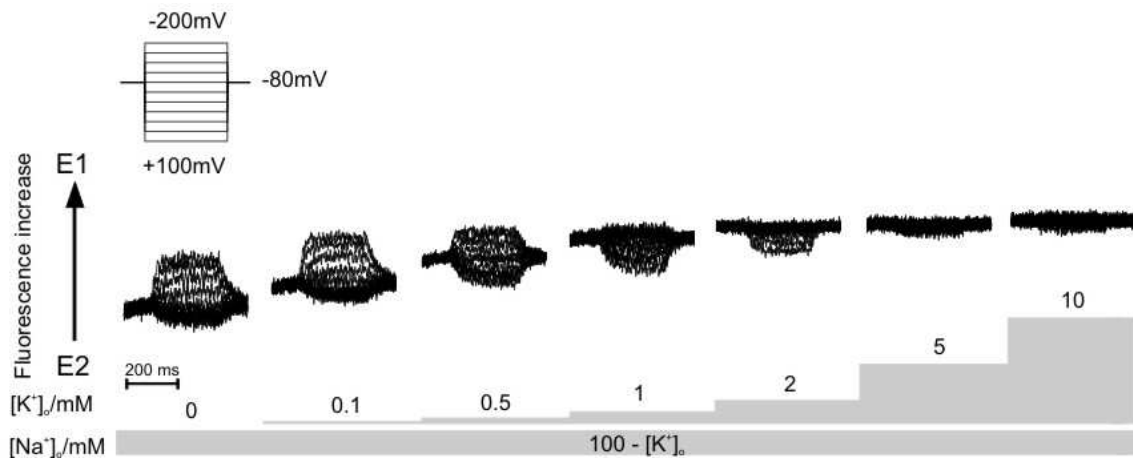**Fig. 3.5: Na$^+$,K$^+$-ATPase Mutant N790C. Effect of incremental substitution of Na^+_o with K^+_o on the E$_1$/E$_2$ equilibrium.** Voltage jump-induced fluorescence changes from a continuous recording of a single oocyte (see step protocol). 100mM Na$^+$ in the external solution were incrementally substituted with equimolar amounts of K$^+$. Fluorescence recordings were aligned according to the increasing background-fluorescence at the holding potential (-80mV).

The progressive changes of the voltage step induced fluorescence relaxations in response to increasing amounts of K$^+$ in a Na$^+$-containing external solution (turnover conditions) are shown in Figure 3.5. As stated above, in the absence of external K$^+$, when only the Na$^+$ branch is accessible, fluorescence signals are mainly evoked by hyperpolarising potentials. When the concentration of extracellular K$^+$ is raised, fluorescence signals are increasingly evoked by depolarising potentials and less by hyperpolarising potentials which documents the growing involvement of the K$^+$ branch and a shift of the conformational equilibrium towards E$_1$ (Geibel et al., 2003). Consequently, at [K$^+$]$_o$ = 0.5 mM fluorescence signals can be observed that are induced upon depolarisation and hyperpolarisation, whereas at [K$^+$]$_o$ = 2 mM only depolarisation potential steps evoke fluorescence responses. In the presence of 10 mM K$^+$, the shift of the conformational equilibrium can be assumed to have progressed to the point where depolarising voltage jumps of the step protocol are no longer sufficient to evoke changes in fluorescence intensity. In line with the voltage jump data, the background fluorescence, measured at -80 mV, increased in a concentration dependent manner during the experiment which indicates the relocation of the equilibrium towards E$_1$ (Geibel et al., 2003).
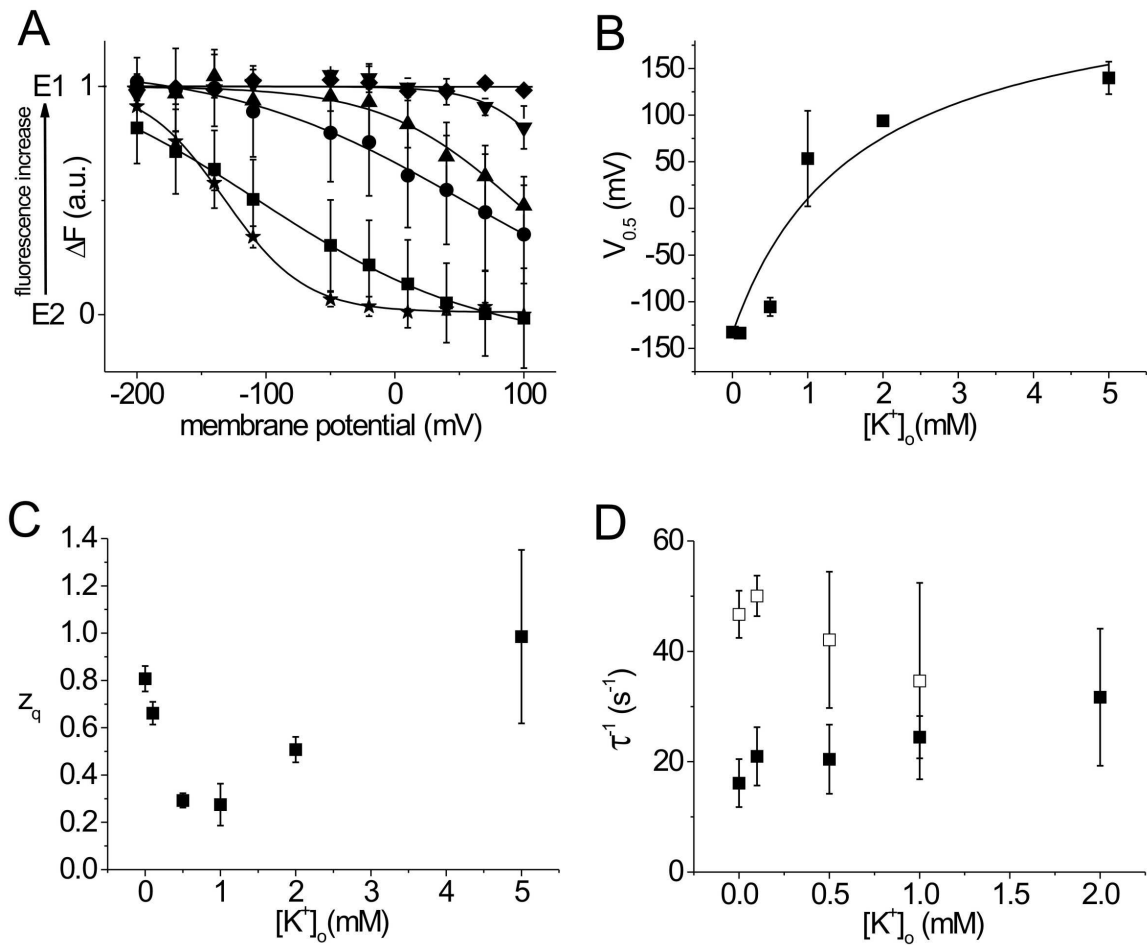
Fig. 3.6: Na$^+$,K$^+$-ATPase Mutant N790C. [K$^+$]$_o$ dependence of the fluorescence changes in the presence of Na^+_o (means ± SD of 3 cells). (A) Voltage dependence of the fluorescence saturation values (including Boltzmann fits). Voltage steps were performed from a holding potential of -80 mV in 30 mV steps to the potentials indicated. The external solution contained, as its main constituent, 100 mM Na$^+$ (ξ), which was successively substituted by 0-10 mM K$^+$ (for the sake of clarity, only data acquired in K$^+$ free solutions (ξ) and at concentrations of 0.5 mM K$^+$ (!), 1 mM K$^+$ (,), 2 mM K$^+$ (7), 5 mM (Β) and 10 mM K$^+$ (Λ) are shown here). **(B)** Midpoint potentials, V$_{0.5}$ (± SE), of the Boltzmann functions. The concentration dependence of the V$_{0.5}$ values can be approximated by a sigmoidal function. **(C)** Apparent translocated charge, z$_q$ (± SE), related to the observed conformational change. **(D)** Apparent rate constants, τ^{-1} (± SD), of the fluorescence relaxations in response to voltage jumps from a holding potential of -80 mV to +100 mV (!) and -200 mV (∀).

Changes in fluorescence intensity

More information can be gained from the K$^+$ dependence of the ΔF-V curves and their corresponding Boltzmann functions as shown in Figure 3.6A (means ± SD of 3 cells). Data were acquired in experiments as displayed in Fig. 3.5 and fluorescence was recorded under Na$^+$/Na$^+$ exchange conditions, as a reference, and under conditions where Na$^+$ was replaced by K$^+$ on an equimolar basis (0.1, 0.5, 1, 2, 5 and 10 mM, respectively, not all data are

shown in 3.6A). The results from these experiments demonstrate that the addition of K^+ produces a shift of the ΔF-V curves towards more depolarising potentials. At 0.5 mM K^+ and 1 mM K^+, the slope of the Boltzmann functions is less steep, which means that there is a reduced electrogenicity. Extrapolation of the Boltzmann functions at 0.1, 0.5 and 1 mM K^+ results in curves that surpass the saturation values of the reference measurement under Na^+/Na^+ exchange conditions (up to a maximum of 1.3 times the reference value at 0.5 mM K^+, respectively). The reason for this increase could be the availability of new enzyme conformations like E_2K and E_1K under turnover conditions that exhibit slightly different changes fluorescence intensity.

The K^+ dependence of $V_{0.5}$ was fitted to a Hill equation and the Hill coefficient was held at 1 (Figure 3.6B). A low apparent affinity ($K_{0.5} = 1.7 \pm 1$ mM) for K^+ in the presence of Na^+ can be observed that is compatible with previous findings obtained from a comparable $\alpha\beta$-heteromer that featured a TMRM labelled β-subunit ($K_{0.5} = 2.8 \pm 0.3$ mM, Dempski et al., 2005).

It is clear that z_q changes as a function of external K^+ (Figure 3.6C). The value of z_q decreases from 0.81 ± 0.05 under Na^+/Na^+ exchange conditions to a value of 0.27 ± 0.09 in the presence of 1 mM K^+. However, in spite of the poor quality of the Boltzmann fits, it seems that at K^+ concentrations of 2 mM and higher, z_q increases again.

Kinetics

The apparent rate constants (reciprocals of time constants) of the fluorescence relaxations show a clear difference in response to depolarising (+100 mV) and hyperpolarising (-200 mV) membrane pulses (Figure 3.6D). Upon depolarisation values oscillate around 20 s^{-1} up to a K^+ concentrations of 1 mM (e.g. 16 ± 4 s^{-1} at 0 mM K^+ and 24 ± 4 s^{-1} at 1 mM K^+), with a slight acceleration visible at 2 mM K^+ (32 ± 12 s^{-1}). In contrast, the apparent rate constants upon hyperpolarisation are clearly accelerated in the absence of K^+ (47 ± 4 s^{-1}) but slow down upon addition of K^+ (35 ± 18 s^{-1} at 1 mM K^+). Hyperpolarisation accelerates Na^+ rebinding and the transition to $E_1(P)$ due to the existence of an external access channel for Na^+. This process seems to become impeded at increasing K^+ concentrations. It was not possible to determine the rate constant for the potential jump to -200 mV at higher K^+ concentrations due to the shift of the ΔF-V curves and the resulting lack of fluorescence relaxations at this potential.

3.3.2 Substitution of external N-methyl-D-glucamine

In another set of experiments, external Na^+ was replaced by NMG^+ more effectively isolate the K^+ branch of the reaction cycle by prohibiting the rebinding of Na^+ (Figure 3.7).
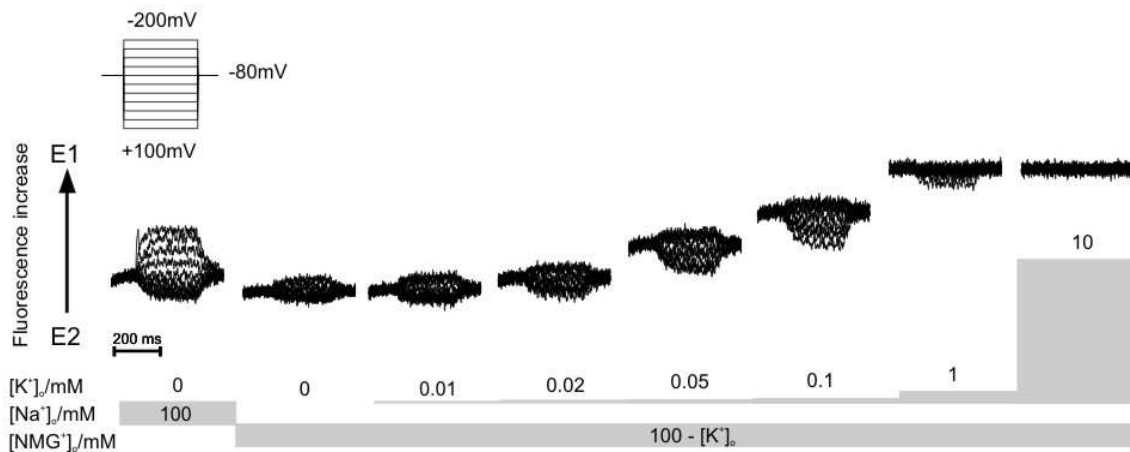

Fig. 3.7: Na^+,K^+-ATPase Mutant N790C. Effect of incremental substitution of NMG^+_o with K^+_o on the E_1/E_2 equilibrium. Voltage jump-induced fluorescence changes from a continuous recording of a single oocyte. 100 mM NMG^+ in the external solution were incrementally substituted with equimolar amounts of K^+. A reference measurement under Na^+/Na^+ exchange conditions is included. Voltage jumps were performed according to the indicated step-protocol and fluorescence recordings were aligned according to the increasing background-fluorescence at the holding potential (-80mV).

First, a reference measurement under Na^+/Na^+ exchange conditions is shown. After switching to a solution containing 100 mM NMG^+, the changes in fluorescence intensity upon voltage jumps are small and might be the result of a residual Na^+ contamination as NMG^+ is not translocated by the ion pump. Upon substitution of small amounts of NMG^+ by K^+ (10, 20, 50 and 100 µM, respectively) the amplitudes of the fluorescence responses evoked by depolarising potentials are increased, but those upon hyperpolarisation are unaffected. At 1 mM K^+ no changes in fluorescence intensity can be observed upon hyperpolarisation and only minor responses are seen upon depolarisation which indicates an equilibrium that mainly rests in E_1. Fluorescence changes are completely absent at 10 mM K^+ because the conformational equilibrium has been relocated thoroughly towards E_1 and depolarising voltage jumps of the step protocol are not sufficient to promote the monitored conformational changes. A concentration dependent increase of the background fluorescence level can be observed that also documents a K^+ induced shift of the equilibrium towards E_1.
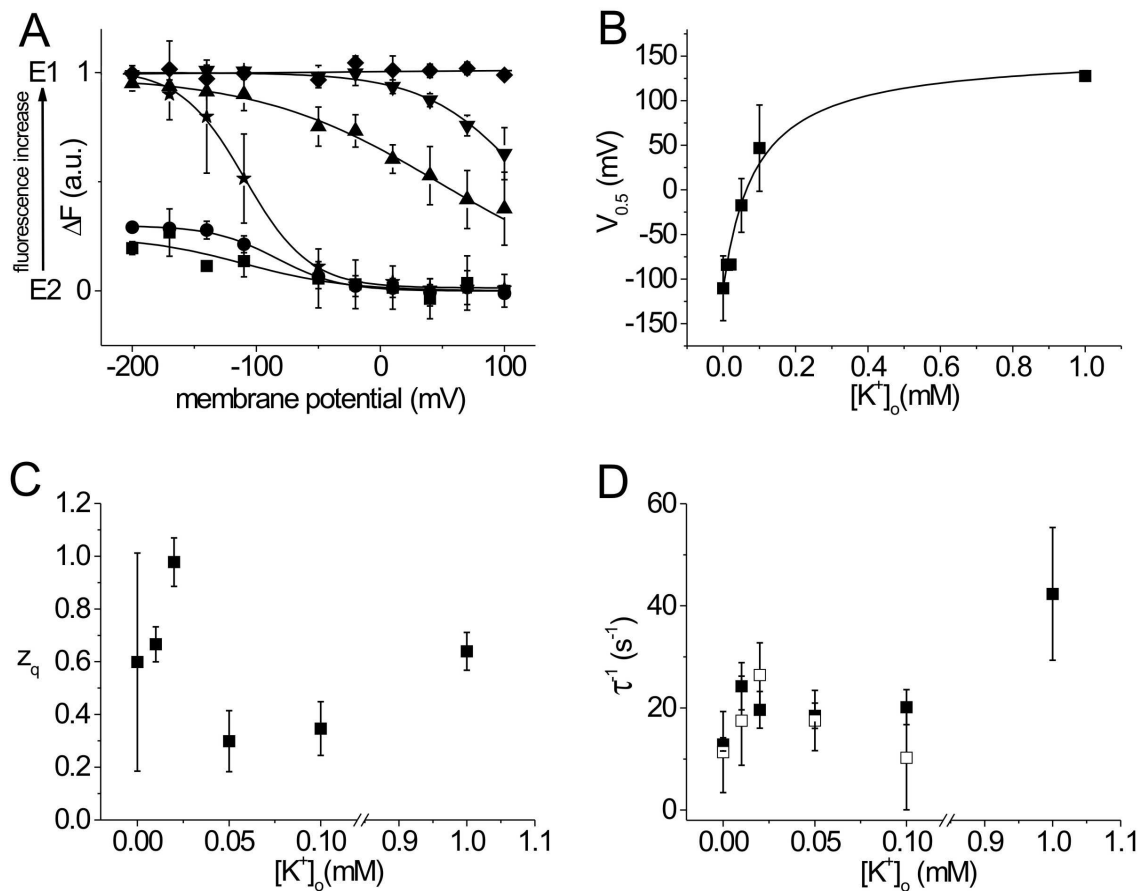
Fig. 3.8: Na$^+$,K$^+$-ATPase Mutant N790C. [K$^+$]$_o$ dependence fluorescence changes in the absence of Na^+_o (means ± SD of 3 cells). (A) Voltage dependence of the fluorescence saturation values and the related Boltzmann functions. Voltage steps were performed from a holding potential of -80 mV in 30 mV steps to the potentials indicated. The external solution contained, as its main constituent, either 100 mM Na$^+$ (ξ), or 100 mM NMG$^+$ (!) substituted with 0-10 mM K$^+$ (for the sake of clarity, only data acquired in K$^+$ free solutions (ξ, !) and at concentrations of 0.02 mM K$^+$ (,), 0.1 mM K$^+$ (7), 1 mM K$^+$ (B) and 10 mM K$^+$ (Λ) are shown here). **(B)** Midpoint potentials, V$_{0.5}$ (± SE), of the Boltzmann functions. The concentration dependence of the V$_{0.5}$ values can be approximated by a monoexponential function. **(C)** Apparent translocated charge, z$_q$ (± SE), related to the observed conformational change. **(D)** Apparent rate constants, τ^{-1} (± SD), of the fluorescence relaxations in response to voltage jumps from a holding potential of -80 mV to +100 mV (!) and -200 mV ($\forall$).

Changes in fluorescence intensity

In Figure 3.8A the K$^+$ dependence of the ΔF-V curves (including the corresponding Boltzmann functions) in the absence of external Na$^+$ is shown. Reference data were obtained under Na$^+$/Na$^+$ exchange conditions, but all other data were acquired in solutions that replaced Na$^+$ by 100 mM NMG$^+$. This was successively substituted by 0, 0.01, 0.02, 0.05, 0.1, 1 and 10 mM K$^+$ on an equimolar basis. Small, voltage dependent fluorescence signals can be observed in NMG$^+$, but might be due to residual contaminations of Na$^+$.

Upon addition of increasing amounts of K^+ the size of the evocable ΔF is increased and the ΔF-V curves are continuously shifted to the right, towards more depolarising potentials. When 0.02 mM NMG^+ are substituted with K^+, the total change in fluorescence intensity given by the amplitude of the Boltzmann function is only about 30% of the respective amplitude under Na^+/Na^+ exchange conditions. However, in the presence of 0.1 mM K^+, the amplitude of the extrapolated Boltzmann function is of comparable size.

The K^+-concentration dependence of the midpoint potential, $V_{0.5}$, of the Boltzmann functions is depicted in Figure 3.8B. The data was fit to a Hill equation and the Hill coefficient held at 1. A high apparent affinity for K^+ in the absence of external Na^+ can be observed ($K_{0.5} = 0.09 \pm 0.02$ mM). This is in agreement with previous results from a comparable $\alpha\beta$ heterodimer with a TMRM labelled β-subunit that were also obtained in NMG^+ based buffer (Dempski et al., 2005).

Figure 3.8C highlights the K^+ concentration dependence on the apparent translocated charge, z_q, that is related to the monitored conformational change. The z_q value in K^+ free solution (0.60 ± 0.41) is difficult to interpret since no transportable ions should be present in the extracellular solution under such conditions. Upon addition of K^+ the z_q value increases at low concentrations of external K^+ and then decreases at slightly higher concentrations of K^+. At $[K^+]_o = 1$ mM it is possible that z_q increases again, but this is hard to determine due to the small portion of the ΔF-V curve that is available for analysis.

Kinetics

As before, two membrane potentials (+100 mV and -200 mV) were selected to display the effect of depolarising and hyperpolarising potentials on the apparent rate constants, τ^{-1}, of the original voltage step induced fluorescence relaxations (Figure 3.8D). Up to a concentration of 0.1 mM K^+ the differences between the two membrane potentials are small and the rate constants oscillate around a value of 20 s^{-1} (upon hyperpolarisation, rate constants between 10.2 ± 10.2 s^{-1} and 26.5 ± 6.3 s^{-1} are calculated; depolarisation results in rate constants between 12.9 ± 1.3 s^{-1} and 24.3 ± 4.6 s^{-1}). Consequently, low concentrations of K^+ do not influence the apparent rate of the monitored conformational transition at either membrane potential. However, a distinct acceleration (42.3 ± 13.0 s^{-1}) can be observed at 1 mM K^+ at +100 mV. No fluorescence signals in response to

hyperpolarisation could be observed at this K^+ concentration and hence it was not possible to determine an apparent rate constant.

3.4 Equivalent effects of $[Na^+]_i$ and $[K^+]_o$ on the conformational equilibrium

When comparing the results from chapter 3.2.1, which depict the effects of low internal Na^+ concentrations on the sodium pump, with data from chapter 3.3.1 or (Geibel et al., 2003) that was obtained in K^+-containing solutions, a resemblance of the effect of low $[Na^+]_i$ and high $[K^+]_o$ on the $E_1(P)/E_2(P)$ equilibrium becomes obvious.
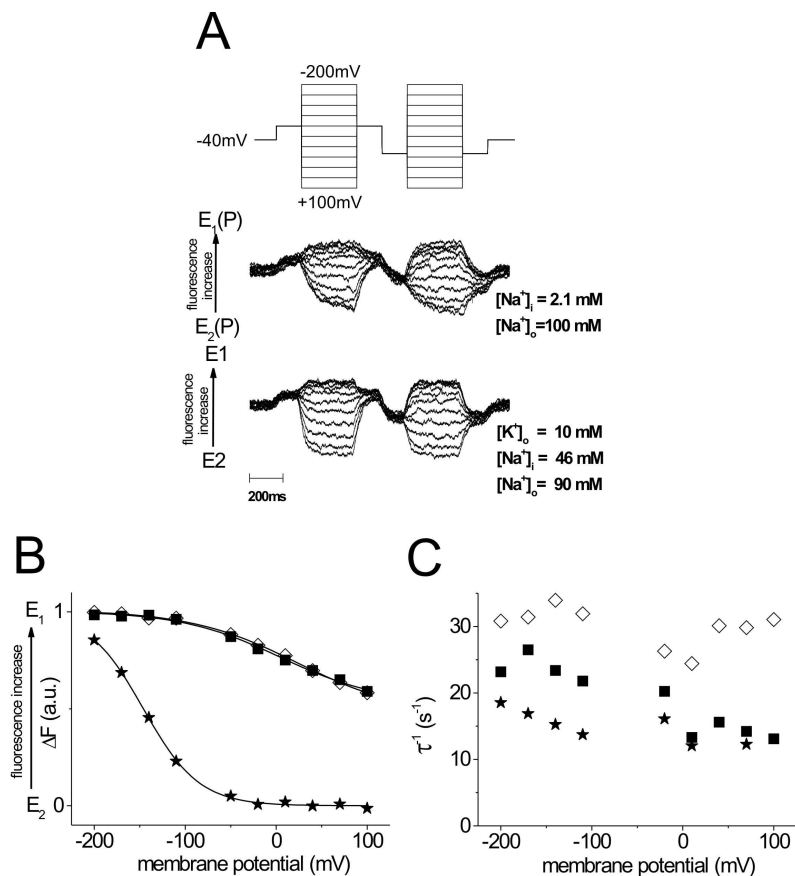
Fig. 3.9: Na^+,K^+-ATPase Mutant N790C. Equivalent effect of $[Na^+]_i$ and $[K^+]_o$ on the E_1/E_2 equilibrium. (A) Original fluorescence recordings of a single oocyte under different ion conditions. **(B)** Voltage dependence of the fluorescence saturation values determined from (A). The main constituents of the solutions are: $[Na^+]_o$ = 100 mM, $[K^+]_o$ = 0 mM, $[Na^+]_i$ = 2.1 mM (!), $[Na^+]_o$ = 90 mM, $[K^+]_o$ = 10 mM, $[Na^+]_i$ = 46 mM (M). Also included is a reference measurement: $[Na^+]_o$ = 100 mM, $[K^+]_o$ = 0 mM, $[Na^+]_i$ = 46 mM (ξ), Boltzmann functions are superimposed. **(C)** Rate constants (reciprocals of time constants) of the fluorescence relaxations. Representation as in (B), two apparent rate constants for (ξ) could not be determined (+100 mV, +40 mV), no apparent rate constants could be determined for the voltage step to -50 mV due to small fluorescence signals.

Changes in fluorescence intensity

Fig. 3.9A shows two original fluorescence recordings obtained in voltage step experiments of a single cell under Na^+/Na^+ exchange conditions: one at very low $[Na^+]_i$ and one under conditions of saturating $[Na^+]_i$ and in the presence of external K^+. The concentrations of the major ions of interest are: $[Na^+]_i = 2.1$ mM, $[Na^+]_o = 100$ mM, $[K^+]_o = 0$ mM for the top recording and $[Na^+]_i = 46$ mM, $[Na^+]_o = 90$ mM, $[K^+]_o = 10$ mM for the bottom recording, respectively. A high degree of similarity between these recordings is obvious. The voltage-step protocol evokes in both cases fluorescence changes in response to depolarising and hyperpolarising potentials which are almost identical in amplitude. The major difference between the two recordings is an apparent acceleration of the fluorescence relaxations in the presence of $[K^+]_o = 10$ mM, which seems to be most prominent at depolarising potentials. It should be noted that oocytes that were previously depleted of Na^+_i seem to have an increased $[K^+]_o$ due to the depletion procedure (see Materials and Methods). This explains the observation of voltage jump induced fluorescence relaxations at $[K^+]_o = 10$ mM which would not be possible under regular conditions (see Fig. 3.5)

The ΔF-V curves of the data in Fig 3.9A along with the Boltzmann approximations are shown in Fig. 3.9B. Also included is a reference measurement performed under standard Na^+/Na^+ exchange conditions and saturating $[Na^+]_i$. As already indicated by the original fluorescence traces, the ΔF values at low $[Na^+]_i$ display an almost identical voltage dependence as those in the presence of K^+_o.

Kinetics

Fig. 3.9C depicts the voltage dependence of the apparent rate constants, τ^{-1}, of the related ΔF data presented in Fig. 3.9B. At a saturating concentration of Na^+_i of about 46 mM the apparent rate constants are accelerated in a typical voltage-dependent manner at hyperpolarising potentials whereas they are slow and voltage independent at depolarising potentials (~ 10 s^{-1}, compare with Fig. 3.4D). In contrast to this observation, at a concentration of $[Na^+]_i = 2.1$ mM the apparent rate constants seem to be accelerated in a more or less voltage independent manner at hyperpolarising potentials (~ 23 s^{-1}), whereas a slow-down takes place at depolarising potentials. In the presence of $[K^+]_o = 10$ mM all apparent rate constants are accelerated to about 30 s^{-1}, irrespective of the potential. However, it should be noted that this is preliminary data that requires further verification.

4. Results – Investigation of the mutant L311C

The second extracellular loop of the sodium pump connects the transmembrane helices TM3 and TM4 is a region of the Na^+,K^+-ATPase that is reported to be involved in controlling the accessibility of the binding sites (Capendeguy et al., 2006). It has been proposed to be part of a hypothesized outer gate of the pump which originates from the "alternating access model" (Artigas & Gadsby, 2003; Pavlov & Sokolov, 2000). Recent structural data on the Na^+,K^+-ATPase (Morth et al., 2007) and SERCA (Olesen et al., 2007) lend support to the idea of an active role of TM3-TM4 in opening and closing the externally facing exit pathway for ions. The mutation L311C situated in the loop region was introduced to gain further information on this structural feature. In addition, it was specifically investigated if this region reacts differently to changes in the intracellular Na^+ concentration than the TM5-TM6 loop region.

4.1 Characterization of L311C
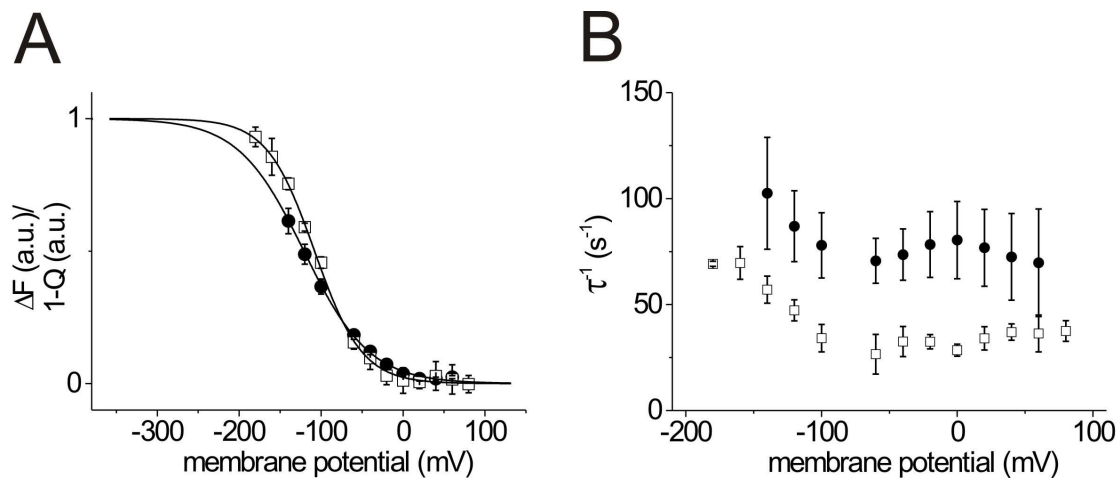
Fig. 4.1: Na$^+$,K$^+$-ATPase Mutant L311C. Electrical and fluorometric characterization. (A) Voltage dependence of the fluorescence saturation values (∀) and the translocated charge (.). The relevant Boltzmann functions are superimposed, yielding the following parameters: $V_{0.5}$ (fluorescence) = -108 ± 2mV, $V_{0.5}$ (charge) = -121 ± 8mV, z_q (fluorescence) = 0.9 ± 0.1, z_q(charge) = 0.6 ± 0.1. **(B)** Rate constants (reciprocals of time constants) of fluorescence changes (∀) and transient currents (.). All data are means ± SD of three cells.

Charge translocation and changes in fluorescence intensity

Fig. 4.1A depicts the voltage dependence of the normalized translocated charge, Q, and the normalized fluorescence saturation values, ΔF, of the reporter complex L311C-TMRM

(means ± SD of three oocytes). Both data sets were approximated by Boltzmann functions. As can be seen from the position of the data points, the changes in fluorescence intensity of the L311C-TMRM sensor complex do not completely overlap with the translocated charge in the potential range between -100 mV to -140 mV. This is also manifested in the divergence of the parameters derived from Boltzmann functions ($V_{0.5}$ (fluorescence) = -108 ± 2 mV, $V_{0.5}$ (charge) = -121 ± 8 mV, z_q (fluorescence) = 0.9 ± 0.1, z_q (charge) = 0.6 ± 0.1). The observed discrepancy might be due to an insufficient number of data points for the translocated charge at hyperpolarising potentials and is probably not crucial. However, this discrepancy has to be kept in mind and attention has to be paid when $V_{0.5}$ and z_q are evaluated.

Kinetics

Fig, 4.1B shows the voltage dependence of the apparent rate constants, τ^{-1}, affiliated with the charge translocation and the fluorescence relaxation (means ± SD of three oocytes, data extracted from monoexponential approximations). Both processes are voltage-independent at depolarising potentials with apparent rate constants amounting to ~ 25 s^{-1} (fluorescence) and ~ 75 s^{-1} (charge) at all potentials, but both are also clearly voltage-dependent at hyperpolarising potentials and apparent rate constants amount to ~ 50 s^{-1} (fluorescence) and ~ 100 s^{-1} (charge) at -140 mV. As could be observed before for the N790C construct, the fluorescence relaxation is a slower process than the charge translocation and seems to be, in the case of L311C, slowed down by about 50 s^{-1} at any given potential.

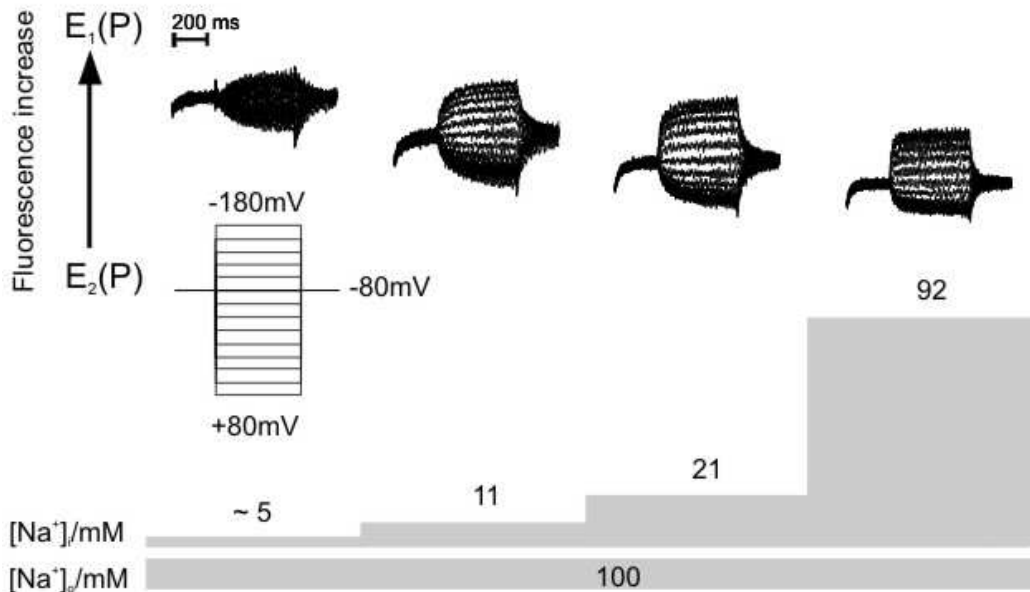# 4.2 Dependence on the internal sodium concentration

Fig. 4.2: Na$^+$,K$^+$-ATPase Mutant L311C. Increase of [Na$^+$]$_i$. Voltage jump-induced fluorescence changes under Na$^+$/Na$^+$ exchange conditions from a continuous recording of a single oocyte at different [Na$^+$]$_i$. Effect on the E$_1$(P)/E$_2$(P) equilibrium. Due to uncompensated fluorophore bleaching the decrease in fluorescence does not quantitate the shift of the conformational equilibrium.

Fig. 4.2 clearly shows that a change of the internal Na$^+$ concentration effects the conformational changes reported by the L311C-TMRM complex. An increase of [Na$^+$]$_i$ leads to an increase of the observed changes in fluorescence intensity which is later reduced by fluorophore bleaching ([Na$^+$]$_i$ = 92 mM). In addition, it can be seen that the fluorescence relaxations are markedly accelerated by the concentration increase. The decrease of the background fluorescence includes the effects of uncompensated fluorophore bleaching and can therefore not be used to quantitate the shift of the equilibrium towards E$_2$(P). However, increasingly larger fluorescence signals are evoked upon hyperpolarisation as [Na$^+$]$_i$ is raised which also speaks for a relocation of the equilibrium in direction of E$_2$(P).

To gain further information the ΔF-V data of three independent VCF experiments (means ± SD) performed under Na$^+$/Na$^+$ exchange conditions were grouped into three concentration intervals representing low (1 - 10 mM, black), medium (10 - 20 mM, red) and high/saturating (20 - 70 mM, green) internal Na$^+$ concentration (Fig. 4.3). All data

were approximated by Boltzmann functions and normalized to the ΔF-V curve acquired under saturating $[Na^+]_i$ conditions (green).
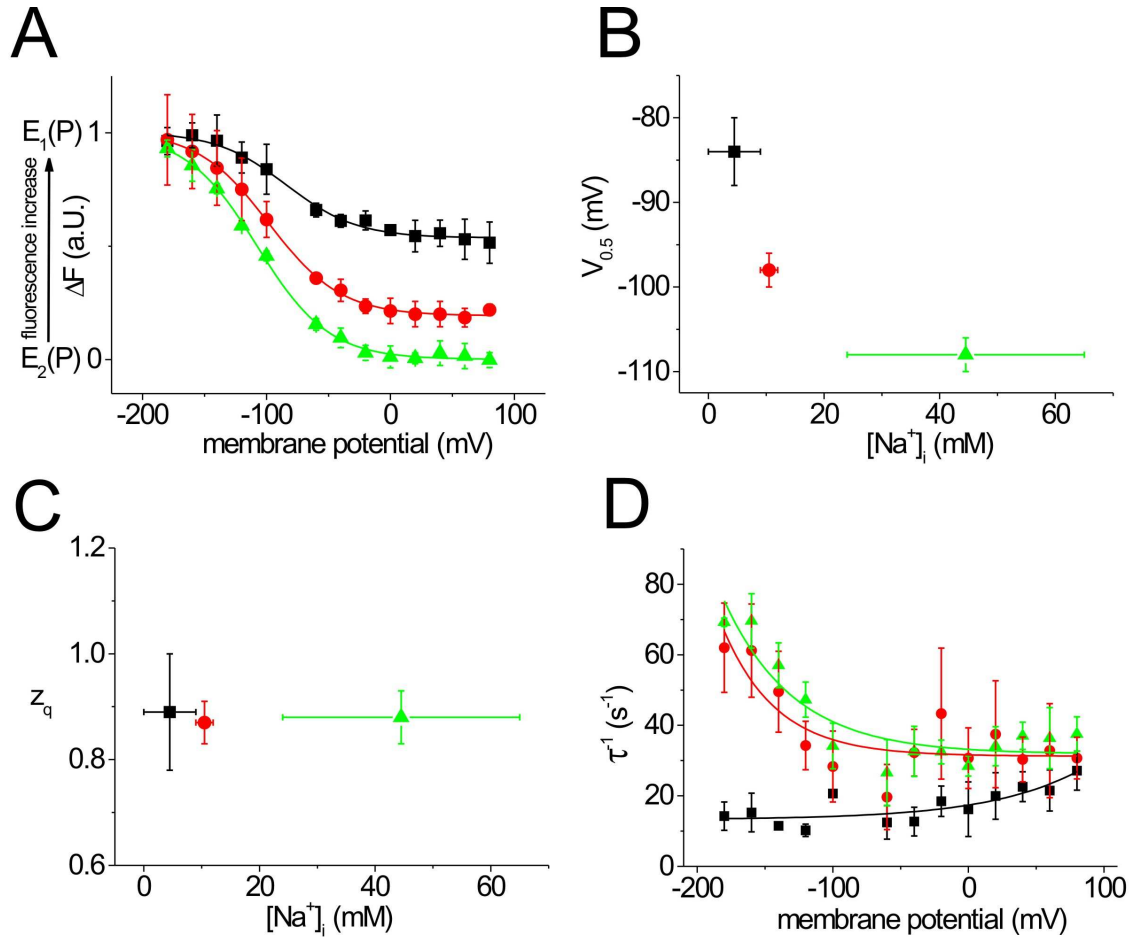
Fig. 4.3: Na⁺,K⁺-ATPase Mutant L311C. [Na⁺]ᵢ concentration intervals. (A) Voltage dependence of the fluorescence saturation values organized into concentration intervals of low (!), medium (.) and saturated (7) $[Na^+]_i$. Data presented as means ± SD of 3 cells and the corresponding Boltzmann functions. All voltage steps were executed from HP = -80 mV. **(B)** Dependence of the midpoint potential $V_{0.5}$ of the Boltzmann finctions on $[Na^+]_i$. Concentration intervals stretch from the minimal to the maximal $[Na^+]$ measured for more precise localization on the x-axes. Data presented are fit parameters of Boltzmann functions and their standard errors. **(C)** Dependence of the apparent translocated charge z_q on $[Na^+]_i$. Representation as in (B). **(D)** Rate constants of the original fluorescence relaxations organized into concentration intervals as in (A). Data presented as means ± SD of 3 cells and the corresponding monoexponential functions.

Changes in fluorescence intensity

Fig. 4.3A shows the averaged ΔF-V data of three independent VCF experiments (means ± SD) performed under Na⁺/Na⁺ exchange conditions that were grouped into three

concentration intervals representing low (1 - 10 mM, black), medium (10 - 20 mM, red) and high/saturating (20 - 70 mM, green) internal Na^+ concentration. All data were approximated by Boltzmann functions and normalized to the ΔF-V curve acquired under saturating $[Na^+]_i$ conditions (green).

The most obvious effect of an increase of $[Na^+]_i$ is an increase of the evocable fluorescence changes, which is reflected in the growing amplitudes of the Boltzmann functions. At low $[Na^+]_i$ this amplitude amounts to about 50% of the final value under saturating conditions. Unlike the fluorescence changes detected in the sensor-complex N790C-TMRM, which display a saturating behavior at depolarising potentials in the experimentally accessible potential-range (compare with Fig. 3.4A), those of sensor-complex L311C-TMRM also get close to saturation at hyperpolarising potentials. An additional difference to N790C is also that jumps from the HP = -80 mV to depolarising potentials can evoke considerably larger fluorescence changes in the L311C construct. These observations suggest that the conformational equilibrium of L311C is generally shifted towards $E_1(P)$.

To establish a more precise concentration dependence for the parameters derived from the Boltzmann fits, the intervals in Fig. 4.3B and C are defined by the actually measured minimal and maximal concentration values.

The midpoint potentials $V_{0.5}$, displayed in Fig. 4.3B, shift with increasing $[Na^+]_i$ about 24 mV towards more depolarising potentials (from -84 ± 4 mV to -98 ± 2mV to -108 ± 2mV). The shift bears resemblance to the shift observed in the N790C construct, but is displaced on the y-axes by about +35 mV.

Fig. 4.3C shows that basically no significant change is observed for z_q, the apparent translocated charge, as the internal sodium concentration rises (z_q = 0.89 ± 0.11, 0.87 ± 0.04, 0.88 ± 0.05 at low, medium and high $[Na^+]_i$, respectively). This stands in clear contrast to the results for N790C.

Kinetics

Fig. 4.3D depicts the voltage dependence of the averaged apparent rate constants, τ^{-1} (means ± SD), in each concentration interval. All data were approximated by monoexponential functions. The most obvious effect of low $[Na^+]_i$ is an absence of a voltage-dependent acceleration of the apparent rate constants at hyperpolarising potentials (-180 mV to -80 mV). All rate constants in this potential range are slowed down to 10-20

s^{-1}. Interestingly, at depolarising potentials, a slight acceleration from ~ 10 s^{-1} at -60 mV to ~ 30 s^{-1} at +80 mV seems to take place. In contrast to these results, at medium and high $[Na^+]_i$, the typical voltage-dependent acceleration of the kinetics at hyperpolarising potentials can be observed (Geibel et al., 2003). The constant relaxation rate of 30 s^{-1} that arises at all depolarising potentials, is accelerated to about 60 s^{-1} at medium $[Na^+]_i$ and to about 70 s^{-1} at high $[Na^+]_i$ at a potential of -180 mV. A difference between the apparent relaxation rates of approximately 10 s^{-1} is maintained at all hyperpolarising potentials and can therefore be attributed quite confidently to the difference in $[Na^+]_i$.

5. Results – Investigation of the mutant E312C

The investigation of E312C construct follows the same motivation as that of L311C construct (see above). A special feature of this glutamate residue is its possible role in controlling the accessibility of the K^+ binding site (Capendeguy et al., 2006). The proposed involvement in this mechanism was also investigated.

5.1 Characterization of E312C
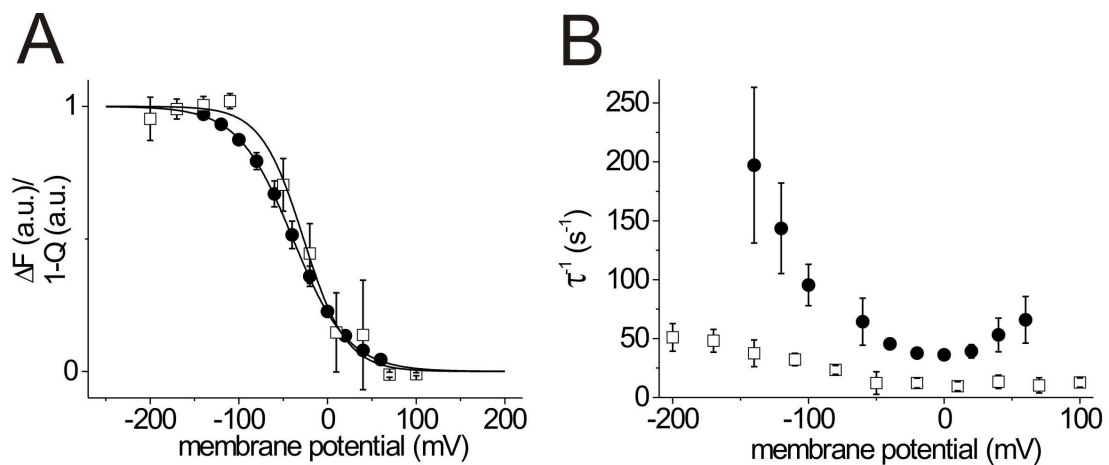
Fig. 5.1: Na$^+$,K$^+$-ATPase Mutant E312C. Electrical and Fluorometric Characterization. (A) Voltage dependence of the fluorescence saturation values (∀) and the translocated charge (.). Normalized VCF data. Fits of the Boltzmann functions are superimposed, yielding the following parameters: $V_{0.5}$ (fluorescence) = -27 ± 4mV, $V_{0.5}$ (charge) = -39 ± 3mV, z_q (fluorescence) = 1.0 ± 0.2, z_q (charge) = 0.81 ± 0.01. **(B)** Rate constants (reciprocals of time constants) of fluorescence changes (∀) and transient currents (.). All data are means ± SD of three cells.

Charge translocation and Changes in fluorescence intensity

The voltage dependence of the normalized translocated charge, Q, and the normalized fluorescence saturation values, ΔF, is shown in Fig. 5.1A. As mentioned before, both normalized data-sets were approximated by Boltzmann functions. It becomes obvious, that in the potential range between -25 mV to -150 mV the Boltzmann functions diverge slightly. This is also represented by the differing midpoint potentials ($V_{0.5}$ (fluorescence) = -27 ± 4 mV, $V_{0.5}$ (charge) = -39 ± 0.3 mV) and the different values for the apparent translocated charge (z_q (fluorescence) = 1.0 ± 0.2, z_q (charge) = 0.81 ± 0.01) determined from the associated Boltzmann functions. Even though these differences do not seem to be crucial they have to be kept in mind in case they are relevant for the interpretation of the

data. Nevertheless, the fluorescence and electrical data are still in reasonably good agreement, so that it can be implied that E312C-TMRM reports the conformational change of the $E_1(P)/E_2(P)$ and that fluorescence signals from this location can be used to gauge the $E_1(P)/E_2(P)$ ratio.

Kinetics

Fig. 5.1B shows the voltage dependence of the apparent rate constants, τ^{-1}, associated with the charge translocation and the fluorescence relaxation of Fig. 5.1A (means ± SD of three oocytes). The charge translocation is the faster of the two processes, as could be expected from the data presented of the N790C construct (see chapter 3.1.1) and the L311C construct (see chapter 4.1). This process seems to be slowest at 0 mV ($\sim$ 40 s^{-1}) but is slightly accelerated at potentials above 0 mV ($\sim$ 65 s^{-1} at + 60 mV) and considerably accelerated at potentials below 0 mV (about 200 s^{-1} at -140 mV). The comparison with the literature (Geibel, 2003) reveals that the voltage dependence and magnitude of the observed charge translocation rate constants of the E312C construct bear the closest resemblance to those of the wild-type sheep Na$^+$,K$^+$-ATPase of all the mutants investigated so far (see also Introduction). In contrast, the fluorescence relaxation is a comparatively slow process at potentials above -50 mV ($\sim$ 10 s^{-1}) but is increasingly accelerated below -50 mV ($\sim$ 50 s^{-1} at -200 mV).

5.2 Dependence on the internal sodium concentration $[Na^+]_i$
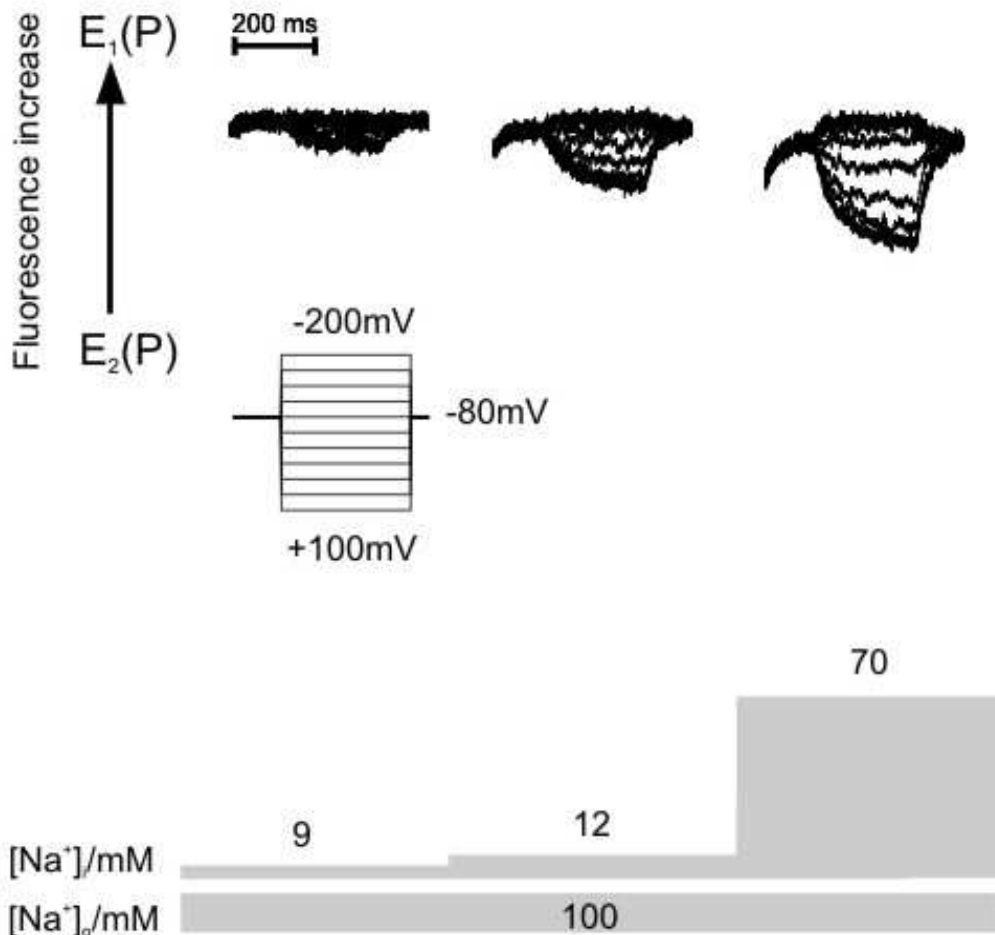
Fig. 5.2: Na^+,K^+-ATPase Mutant E312C. Increase of $[Na^+]_i$. Voltage jump-induced fluorescence changes under Na^+/Na^+ exchange conditions from a continuous recording of a single oocyte at different $[Na^+]_i$. Effect on the $E_1(P)/E_2(P)$ equilibrium. Fluorophore bleaching was compensated for manually, therefore the shift in background fluorescence could not be determined from these recordings.

Increasing the concentration of internal Na^+ does not seem to have a major impact on the conformational equilibrium of E312C under Na^+/Na^+ exchange conditions (Fig. 5.2). Even though an obvious increase of the fluorescence signals can be observed, the continuous recordings show that at any $[Na^+]_i$ fluorescence responses are mainly evoked by steps to depolarising potentials. This accounts for a conformational equilibrium that is heavily shifted towards $E_1(P)$. Only at high $[Na^+]_i$ small fluorescence relaxations can be observed upon jumps to hyperpolarising potentials. No information on the shift of the background fluorescence could be gained from this specific experiment. Other experiments generally

suggest a very minor shift towards $E_2(P)$. However, since the decrease in background fluorescence is so small it cannot be ruled out that a shift to $E_1(P)$ takes place that is negated by fluorophore bleaching.
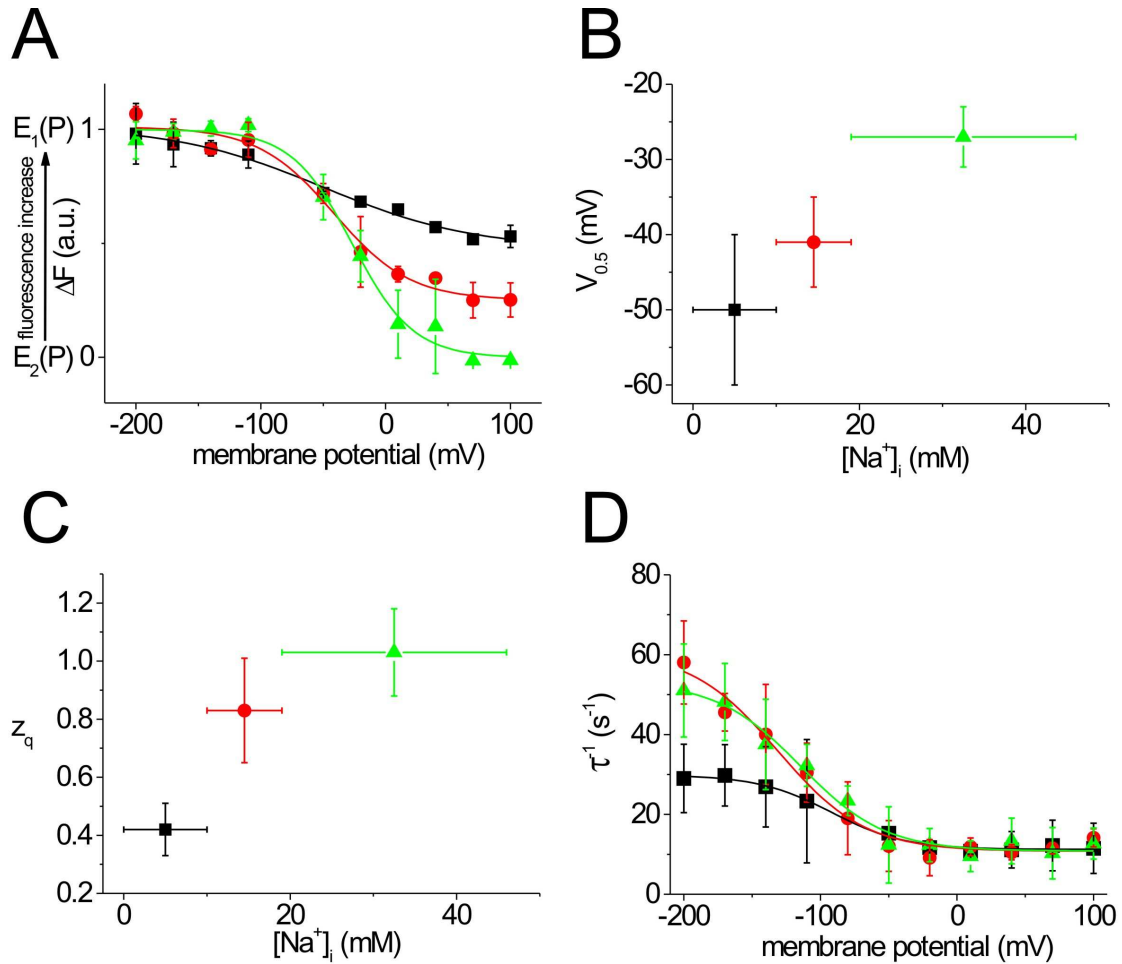
Fig. 5.3: Na^+,K^+-ATPase Mutant E312C. $[Na^+]_i$ concentration intervals. (A) Voltage dependence of the fluorescence saturation values organized into concentration intervals of low (!), medium (ˌ) and saturated (7) $[Na^+]_i$. Data presented as means ± SD of 3 cells and includes corresponding Boltzmann fits. All voltage steps were executed from HP = -80mV. **(B)** Dependence of the midpoint potential $V_{0.5}$ of the Boltzmann functions on $[Na^+]_i$. Concentration intervals stretch from the minimal to the maximal $[Na^+]$ measured for more precise localization on the x-axes. Data presented as fit-parameters of Boltzmann functions and their standard errors. **(C)** Dependence of the apparent translocated charge z_q on $[Na^+]_i$. Representation as in (B). **(D)** Apparent rate constants of the fluorescence changes organized into concentration intervals as in (A). Data presented as means ± SD of 3 cells and the corresponding sigmoidal functions.

Changes in fluorescence intensity

As before, the averaged ΔF-V data of three independent VCF experiments (means $\pm$ SD) performed under Na^+/Na^+ exchange conditions was grouped into three concentration intervals representing low (1 - 10 mM, black), medium (10 - 20 mM, red) and high/saturating (20 - 70 mM, green) internal Na^+ concentration (Fig. 5.3A). All data were approximated by Boltzmann functions and normalized to the ΔF-V curve acquired under saturating $[Na^+]_i$ conditions (green). Similar to the results obtained for the sensor-complexes N790C-TMRM and L311C-TMRM, an increase of $[Na^+]_i$ increases the amplitudes of the evocable fluorescence changes of E312C-TMRM. This is clearly depicted by the growing amplitudes of the Boltzmann functions. The investigated potential range (+100 mV to -200 mV) is basically sufficient to achieve the maximally possible fluorescence changes upon de- and hyperpolarisation (except at low $[Na^+]_i$). Notably, in the case of the E312C construct, depolarising potentials evoke much larger fluorescence changes than hyperpolarising potentials at all $[Na^+]_i$, which is especially apparent at high concentrations of internal Na^+, where roughly 90% of the evocable fluorescence change can be generated by a voltage step from the HP = -80 mV to +70 mV or +100 mV.

Contrasting to previous observations for the N790C and L311C constructs, increasing $[Na^+]_i$ shifts the $V_{0.5}$ of E312C by about 23 mV towards more depolarising potentials ($V_{0.5}$ = -50 $\pm$ 10 mV, -41 $\pm$ 6 mV, -27 $\pm$ 4 mV at low, medium and high $[Na^+]_i$, respectively) and not towards more hyperpolarising potentials (Fig. 5.3B).

As shown in Fig. 5.3C, a corresponding $[Na^+]_i$-related increase for z_q can be reported (z_q = 0.42 $\pm$ 0.09, 0.83 $\pm$ 0.18, 1.03 $\pm$ 0.15 at low, medium and high $[Na^+]_i$, respectively) which is similar to the concentration dependence of z_q for the N790C construct.

Kinetics

Fig. 5.3D shows the particular apparent rate constants, τ^{-1} (means $\pm$ SD of three oocytes), related to the fluorescence saturation values in Fig, 5.3A. All data were approximated by sigmoidal functions due to the clearly saturating behavior at depolarising and hyperpolarising potentials. At potentials ranging from -20 mV to +100 mV, the apparent rate constants are not affected by $[Na^+]_i$ and average out to ~10 s^{-1}. Below -20 mV, the apparent rate constants are voltage dependent and general tendency to saturate at very

hyperpolarising potentials can be observed. Increasing $[Na^+]_i$ clearly leads to an acceleration of the monitored process.

5.3 Effect of external potassium $[K^+]_o$

To address the question of the involvement of residue E312 in K^+_o-binding experiments were performed on the E312C construct which substituted K^+_o for Na^+_o, in analogy to section 3.3.1.
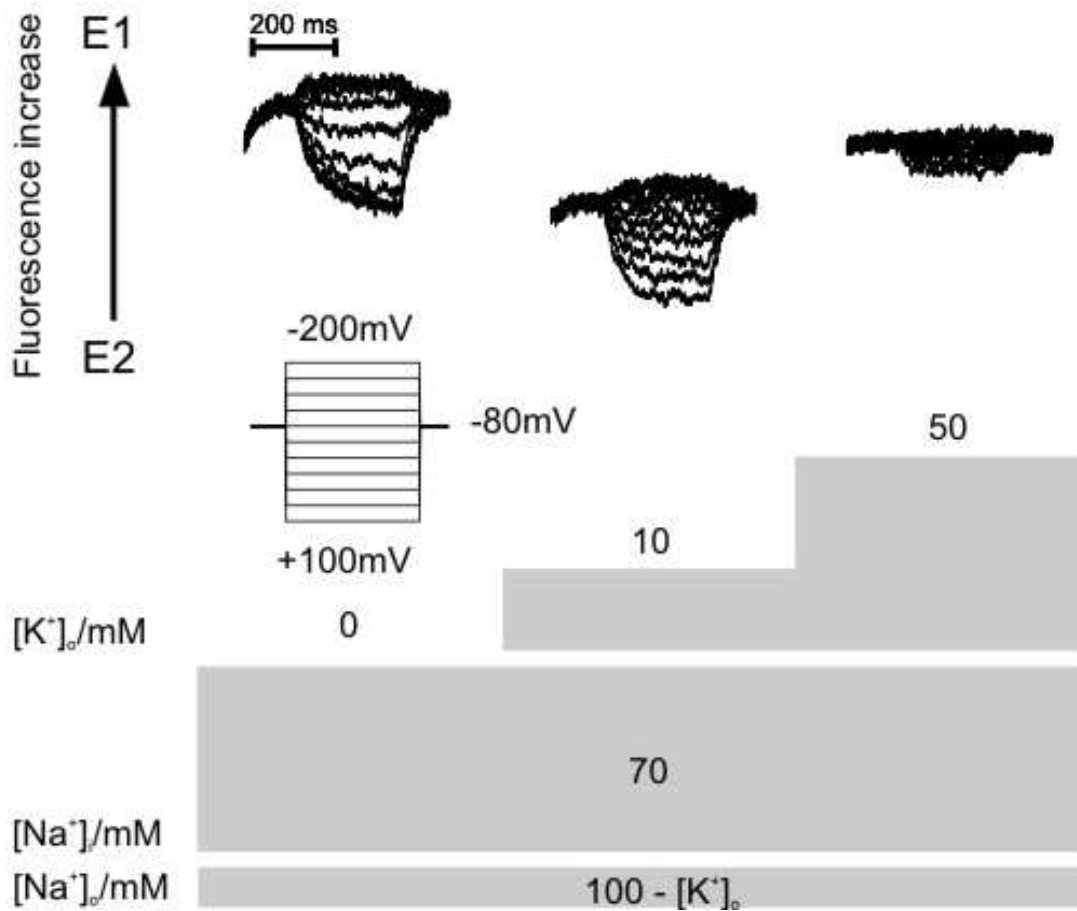
Fig. 5.4: Na^+,K^+-ATPase Mutant E312C. Substitution of Na^+_o with 10 mM K^+_o and 50 mM K^+_o - effect on the E_1/E_2 equilibrium. Voltage jump-induced fluorescence changes from a continuous recording of the same oocyte as in Fig. 5.2. The relative shift in background fluorescence at each K^+ concentration was averaged from eight independent recordings.

The recordings displayed in Fig. 5.4 depict fluorescence data from successive VCF experiments on one oocyte. Voltage step protocols were applied under Na^+/Na^+ exchange conditions and after substituting fractions of external Na^+ by 10 mM K^+ and 50 mM K^+, respectively. In the presence of 100 mM Na^+ fluorescence responses of the E312C-TMRM

sensor complex are mainly evoked by jumps to depolarising potentials. Upon depolarisation to about +40 mV saturation of the fluorescence signals is already reached. In the presence of 10 mM K$^+$ the fluorescence relaxations look very similar, but they do not saturate upon depolarisation and they are apparently accelerated. Furthermore, the level of the background fluorescence is clearly reduced. Addition of 50 mM K$^+$ reduces the size of the evocable fluorescence responses and restricts them to depolarising potentials. The shift of the background fluorescence is not as substantial as upon the addition of 10 mM K$^+$.
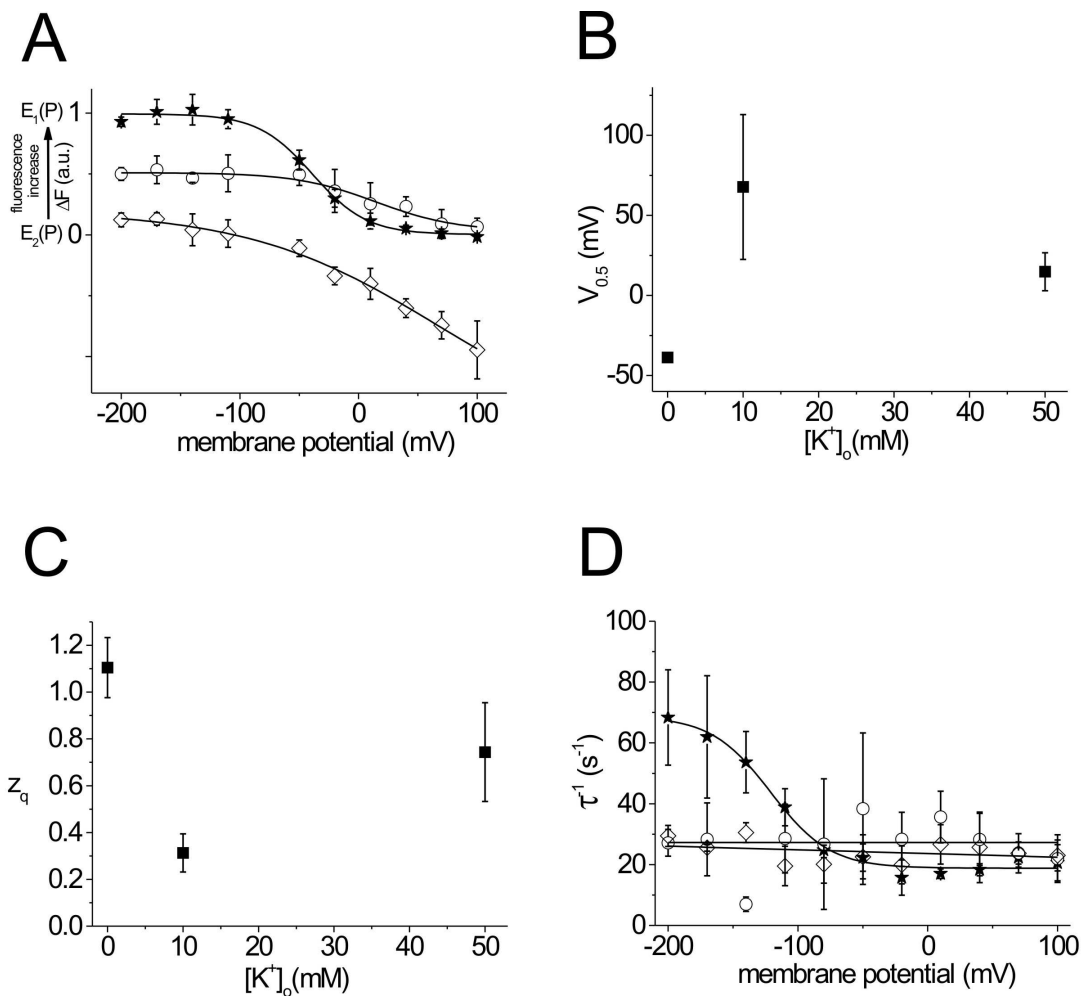
Fig. 5.5: Na$^+$,K$^+$-ATPase Mutant E312C: K$^+$-substitution of external Na$^+$. (A) Voltage dependence of the fluorescence saturation values at increasing [K$^+$]$_o$. Experiments were performed under Na$^+$/Na$^+$ exchange conditions, but the main constituent of the external solution (100 mM Na$^+$, (ξ)) was subsequently replaced by equimolar amounts of K$^+$ (10 mM K$^+$ (M) and 50 mM K$^+$ (−), respectively). Curves reflect best approximation of these data by a Boltzmann function and were aligned according to the levels of background fluorescence in Fig. 5.4. Data are presented as means ± SD of 3 cells. **(B)** Dependence of the midpoint potential, V$_{0.5}$, on [K$^+$]$_o$. Values of V$_{0.5}$ were obtained from the corresponding Boltzmann functions and are shown with their respective standard errors. **(C)** Dependence of the apparent translocated charge z$_q$ on [K$^+$]$_o$. Representation as for V$_{0.5}$. **(D)** Apparent rate constants of the original fluorescence relaxations. Representation as in (A).

Changes in fluorescence intensity

Fig. 5.5A shows the averaged ΔF-V data of three independent VCF experiments (means $\pm$ SD) performed under Na^+/Na^+ exchange conditions and under conditions, in which the main constituent of the solution (100 mM Na^+) was subsequently replaced by 10 mM and 50 mM K^+ on an equimolar basis. Data were approximated by use of a Boltzmann function and normalized to the data acquired under Na^+/Na^+ exchange conditions.

Obviously, the voltage dependence of the ΔF values changes upon addition of 10 mM K^+ and the accessible voltage range is by far not enough to obtain saturation of ΔF upon depolarisation. In addition, the total amplitude of the Boltzmann distribution seems to be considerably increased after addition of $[K^+]_o = 10$ mM. Interestingly, the background fluorescence was substantially reduced.

In contrast, addition of $[K^+]_o = 50$ mM leads to smaller fluorescence changes in respect to the reference. It cannot be determined without doubt if the ΔF-V curve is of sigmoidal shape. However, the reduction in background fluorescence is markedly less than after addition of 10 mM K^+.

The midpoint potential, $V_{0.5}$, is shifted to more depolarising potentials as the external K^+ concentration is increased (Fig. 5.5B). However, due to a lack of data points the exact relationship cannot be described.

In good analogy with the N790C-TMRM data, z_q decreases with an increasing K^+ concentration (Fig. 5.5C).

Kinetics

Fig 5.5D shows the particular apparent rate constants, τ^{-1}, of the data presented in Fig. 5.5A. In the presence of 100 mM Na^+, the previously observed concentration dependence of the rate constants obtained at E312C-TMRM is displayed (see Fig. 5.3D). The addition of 10 mM and 50 mM K^+ abolishes the voltage dependence of the rate constants completely and fixes them at constant 25 - 30 s^{-1} for both concentrations. This finding matches the result for the effect of K^+_o on the N790C construct in Fig. 3.9C.

6. Discussion

The aim of the present study was to investigate the structure-function relationship of two important loop regions of the Na^+,K^+-ATPase: (i) The second extracellular loop between the helices TM3 and TM4, which has been implicated in ion access and egress to the binding pocket located in the inner membrane area of the pump (Eguchi et al., 2005) and (ii) the third extracellular loop between TM5 and TM6, which is close to the ion egress site and located at the exterior end of the piston-like TM5 helix that connects the ion binding region with the intracellular site of ATP binding and protein phosphorylation.

In order to investigate substrate-related conformational rearrangements in these two loop regions, the effects of changes in the concentration of internal Na^+ and/or external K^+ were studied. It was possible to reveal the impact of these ions on the functional mode of the pump by combining an electrophysiological assay in combination with additional, site-specific fluorescence reporters (Voltage Clamp Fluorometry assay, VCF).

6.1 Coexpression of ENaC does not change the properties of the Na^+,K^+-ATPase

The experiments in the present study, which combine the expression of ENaC and the Na^+,K^+-ATPase, confirm that after using ENaC to load the oocytes to a saturating concentration of Na^+_i, the K^+_o-induced pump currents and the fluorescence signals from VCF experiments generally match signals obtained under comparable conditions without coexpression of ENaC (Fig. 3.2 A, B). The method of coexpressing ENaC with the Na^+,K^+-ATPase to manipulate the concentration of intracellular Na^+ has been previously applied (Crambert et al., 2000; Hasler et al., 1998; Horisberger & Kharoubi-Hess, 2002) and no compromising effects on the properties of the Na^+,K^+-ATPase have been reported. The experiments within this thesis suggest that the apparent K^+ affinity might be slightly reduced after cells were subjected to the sodium depletion conditions and underwent a series of Na^+-loading experiments (Fig. 3.9A). A possible explanation for this might be that there is an increase of the intracellular K^+ concentration during the Na^+_i depletion process due to the increased pump activity. Yet, in the oocyte system it can also not be excluded that different batches of oocytes differ somewhat in their internal ion content (Weber, 1999). In addition, during very long experiments involving ion pumps or channels a noticeable change of the internal ion composition can occur (Nakao & Gadsby, 1989).

The small change in apparent K^+ affinity described above was only observed in a few and exceptionally long-lasting experiments. Considering the successful application of this method reported in the literature, it can be also be concluded from the present study that the coexpression of ENaC along the Na^+,K^+-ATPase in principle does not change the properties of the Na^+,K^+-ATPase.

6.2 Fluorescence probes on residues L311C and E312C monitor the $E_1(P)/E_2(P)$ equilibrium

The Q-V and ΔF-V relationships of both sensor complexes L311C-TMRM and E312C-TMRM exhibit a high degree of similarity under Na^+/Na^+ exchange conditions (see chapters 3.1.1, 4.1 and 5.1). This can be taken as a strong indication that fluorescence changes of these sensor complexes reflect the state distribution of the ion pump. Under Na^+/Na^+ exchange conditions, the monitored conformational change is directly correlated to the main electrogenic step in the transport cycle, which is the release or reuptake of Na^+ on the extracellular side of the pump (Nakao & Gadsby, 1986). This electrogenic step is voltage-dependent and the application of depolarising or hyperpolarising potentials influences the position of the $E_1(P)/E_2(P)$ equilibrium up to maximum accumulation of the enzyme in the corresponding state. Changes in fluorescence intensity recorded in parallel with transient currents document the structural rearrangement during the conformational transition. As for the charge translocation, the apparent rate constants of the fluorescence relaxations are voltage dependent and the fluorescence saturation values likewise report the accumulation of either $E_1(P)$ or $E_2(P)$ (Geibel et al., 2003).

In the VCF experiments under Na^+/Na^+ exchange conditions the midpoint potentials, $V_{0.5}$, of Q-V and ΔF-V curves obtained for L311C-TMRM and E312C-TMRM as determined from Boltzmann fits to the data were -121 ± 8 mV *versus* -108 ± 2 mV and -39 ± 3 mV *versus* -27 ± 4 mV, respectively. The information about the conformational equilibrium that can be gained from both reporter positions is therefore virtually identical for Q-V and ΔF-V data. It should be noted though, that the introduction of the cysteine mutations themselves has an impact on the position of the $E_1(P)/E_2(P)$ equilibrium. Judging from the $V_{0.5}$ of the Q-V relationship of the wild type (-71 ± 9 mV) (Geibel, 2003), the equilibria of N790C (-110 ± 9 mV) and L311C (-121 ± 8 mV) are shifted towards $E_2(P)$,

whereas that of E312C (-39 ± 3 mV) is shifted towards $E_1(P)$. Naturally, the same is true for the ΔF-V relationships.

The apparent translocated charge, z_q, of L311C-TMRM and E312C-TMRM determined using ΔF-V and Q-V data differs more strongly (0.9 ± 0.1 *versus* 0.6 ± 0.1 for L311C-TMRM and 1.0 ± 0.2 *versus* 0.81 ± 0.01 for L312C-TMRM, respectively). Yet, at least in the case of sensor complex L311C-TMRM, the variance in z_q probably only mirrors the less-well defined Q-V curve slope (see Fig. 4.1A). Another origin of the difference may be based on a variance in cytosolic ion concentrations, because different oocyte batches were used for the transient current recordings and the fluorescence measurements (Weber, 1999).

Nevertheless, as in N790C-TMRM, the similarly voltage-dependent kinetics of the charge translocation and fluorescence relaxations (Fig. 4.1B and Fig. 5.1B) are a good indication that the fluorescence changes reflect the state transition of the pump and can be used to determine the concentrations of $E_1(P)$ and $E_2(P)$. In addition, the apparent rate constants of the fluorescence relaxations show that the conformational changes monitored by L311C-TMRM and E312C-TMRM are faster than that monitored by N790C-TMRM, which makes these reporter positions more suitable for kinetic studies.

6.3 VCF visualizes conformational states of the K^+ branch

Upon addition of small amounts of K^+ to a Na^+ containing extracellular solution an increase of the amplitudes of the N790C-TMRM ΔF-V curves in comparison to Na^+/Na^+ exchange conditions can be observed (Fig. 3.6A). It cannot be determined if this is a transient or persistent effect, because at higher concentrations of K^+ the fluorescence increase might be covered by the pronounced shift of the ΔF-V curves towards more depolarising potentials. This shift gradually pushes the ΔF-V curves out of the accessible potential range so that at some point the overall change in fluorescence cannot be resolved.

Under Na^+/Na^+ exchange conditions voltage jumps redistribute the $E_1(P)/E_2(P)$ equilibrium in a saturating manner which can be determined using the Q-V relationship of the translocated charge (Rakowski, 1993). Geibel et al., 2003 demonstrated in VCF experiments, that this redistribution is paralleled by the changes in fluorescence intensity of TMRM seen during the conformational change that is closely associated with the charge

translocation. Therefore, the sigmoidal ΔF-V distribution can be also be used to measure the ratio of $E_1(P)$ and $E_2(P)$.

A possible explanation for an increase in fluorescence upon addition of K^+ can be found in recent data on the pump cycle of SERCA (Olesen et al., 2007). It seems quite likely that the structural rearrangements that open the external exit pathway for Na^+ release in the Na^+,K^+-ATPase are not exactly the same as those that close the pathway for K^+ occlusion. The environmental changes that the dye senses will therefore differ. Hence it is not surprising that the changes in fluorescence intensity that accompany the $E_1(P)/E_2(P)$ transition of the Na^+ branch are not exactly of the same magnitude or follow the same kinetics as those that accompany the E_2/E_1 transition of the K^+ branch. In addition, it has to be considered that in the presence of K^+ and Na^+ several different conformations with different fluorescence intensities contribute to the fluorescence signal, presumably until saturation is reached. However, the data acquired at high external K^+ concentrations in the presence of Na^+ and in the absence of Na^+ are very similar. This suggests that the observed fluorescence signals can mainly be attributed to conformational changes in the K^+ branch (Fig. 3.6, Fig. 3.8).

6.4 External Na^+ and K^+ influence the conformational equilibrium

From the VCF experiments on N790C-TMRM in chapter 3.3 it can be inferred, that the apparent affinity for external K^+ is higher in solutions that do not contain Na^+ (Nakao & Gadsby, 1989). This is clearly manifested in the K^+ induced shift of the conformational equilibrium to E_1, since comparable fluorescence responses can be evoked at about five - to tenfold lower K^+ concentrations if the external solution is free of Na^+ (Fig. 3.5 and 3.6A, Fig. 3.7 and 3.8A,). In addition, it takes less K^+ to shift the midpoint potentials of the ΔF-V curves towards more positive potentials (Fig. 3.6B, Fig. 3.8B).

Furthermore, the kinetics of the fluorescence changes also reflect the impact of the ion composition of the external solution on the conformational equilibrium (see Fig. 3.6D and Fig. 3.8D). If Na^+ is present at low external K^+ concentrations ($[K^+]_o = 0 - 0.1$ mM), the apparent rate constants of the fluorescence relaxation are accelerated upon hyperpolarisation to -200 mV (~ 48 s^{-1}), but not upon depolarisation to +100 mV (~ 19 s^{-1}). Under these conditions, hyperpolarisation promotes Na^+ rebinding and the conformational change to $E_1(P)$ via the Na^+ branch due to the existence of an external access channel

(Gadsby et al., 1993). At higher external K^+ concentrations the apparent rate constant upon hyperpolarisation decreases until it matches up with the slightly accelerated apparent rate constant for depolarisation (~ 30 s^{-1}). Na^+ rebinding is at this point no longer promoted in a specifically voltage dependent fashion and the conformational equilibrium is shifted in favor of the K^+ branch and the E_2/E_1 transition. Correspondingly, experiments in Na^+-free solution exhibit both at hyperpolarising and depolarising voltage-steps rate constants of $\sim$ 19 s^{-1} in the presence of $0 - 0.1$ mM K^+.

6.5 The reduction of the internal Na^+ concentration equals an increase of the external K^+ concentration

The $[Na^+]_i$-dependent change of the fluorescence signals of N790C-TMRM under Na^+/Na^+ exchange conditions observed at low $[Na^+]_i$ (see chapter 3.3; Fig. 3.3A) suggests a change of the $E_1(P)/E_2(P)$ equilibrium from $E_2(P)$ under saturating conditions towards $E_1(P)$ at low $[Na^+]_i$. This is based on the observation that at a high internal Na^+ concentration of 13.5 mM and greater, fluorescence signals are mainly evoked by hyperpolarising potentials, which promote the $E_1(P)$ conformation, whereas at low $[Na^+]_i$ of 1.0 mM fluorescence signals are limited to depolarising potentials which promote $E_2(P)$. Furthermore, the $V_{0.5}$ of Boltzmann fits to the fluorescence data is significantly shifted to more positive potentials as the internal Na^+ concentration is lowered. Such a shift also indicates a substantial relocation of the $E_1(P)/E_2(P)$ equilibrium toward the $E_1(P)$ conformation.

In all, the $[Na^+]_i$-dependent change of the voltage step-induced fluorescence signals in chapter 3.2 shows a close resemblance to the $[K^+]_o$-dependent change of the fluorescence signals described in chapter 3.3 and observed by (Geibel et al., 2003). Both can be interpreted as an incremental shift of the conformational equilibrium from $E_2(P)$ to $E_1(P)$ or from E_2 to E_1, respectively. Hence, this high similarity suggests that an increase of $[K^+]_o$ influences the position of the equilibrium in a comparable way as a decrease of $[Na^+]_i$ (see also Fig. 3.9 A, B) and both conditions shift the equilibrium towards $E_1(P)$. Recent data on the pump cycle of SERCA (Olesen et al., 2007) make it seem likely that the structural rearrangements that open the external exit pathway for Na^+ release in the Na^+,K^+-ATPase are not exactly the same as those that close the pathway for K^+ occlusion. Therefore, it is not surprising that the magnitude of the fluorescence changes and the apparent rate constants are different. Furthermore, a mixture of conformations has to be expected as soon as K^+ is present in the external solution.

Another indication for an analogous effect of low $[Na^+]_i$ and high $[K^+]_o$ is given in Fig. 3.11C. The voltage-induced fluorescence relaxations observed at a physiological internal Na^+ concentrations are accelerated to roughly 30 s^{-1} after subjecting the cells to a high external K^+ concentration ($[K^+]_o$ = 10 mM). The data show, that this acceleration is at least partly mirrored if cells are measured under external K^+-free conditions and subjected to a low internal Na^+ concentration of around 2.1 mM. However, since these experiments provided only preliminary data, the true extent of the kinetic similarities needs further scrutiny.

6.6 Indications that K^+ translocation is electrogenic and ion binding is promoted via an ion well

The observation of voltage dependent fluorescence changes upon addition of K^+ to a Na^+ free NMG^+ solution leads to the following conclusion: K^+ translocation from E_2 to E_1 is voltage dependent. Considering the absence of external Na^+, Na^+ rebinding and the connected voltage dependent conformational transition back from $E_2(P)$ to $E_1(P)$ via the Na^+ branch should be almost impossible due to the fast diffusion of Na^+ away from the binding sites when $E_2(P)$ is reached. In addition, the presence of external K^+ should strongly drive the progression of the pump cycle along the E_2/E_1 conformational transition of the K^+ branch. Therefore it can be assumed that the voltage dependent changes in fluorescence intensity upon hyperpolarisation that can be observed up to a K^+ concentration of 0.1 mM are a result of the electrogenicity of the K^+ branch. The fluorescence relaxations disappear at higher K^+ concentrations due to the shift of the ΔF-V curves towards depolarising potentials. However, this shift shows that the conformational equilibrium, which can be assumed to be mainly set up via the K^+ branch, depends not only on the membrane potential but as well as on the K^+ concentration. This, in turn, suggests that K^+ binds in an ion well.

Generally, K^+ translocation is not thought to be voltage dependent (Gadsby et al., 1989). However, in agreement with our findings, Rakowski et al., 1991 report a pump I-V relationship with a negative slope in Na^+ free solution at sub-saturating K^+ concentrations. They propose that under these conditions hyperpolarisation increases the effective K^+ concentration at the binding sites via an ion well. Yet, the pump operates independently of the voltage when the K^+ concentration has reached a saturating level.

Recent structural data shows the opening and closing of a luminal exit pathway during the pump cycle of SERCA (Olesen et al., 2007). Due to the high structural homology with SERCA the existence of an equivalent external ion pathway can be expected for the sodium pump. Minor structural alterations or changes in the electrostatic landscape might transform the access channel for Na^+ rebinding into an access channel for K^+ binding. However, it is also possible that the properties of the access channel itself are not changed very much and both types of ions can be accumulated in the ion well. Instead, the ion affinities of the binding sites might be modulated to determine which type of ion is transported in the end.

6.7 Indications for the existence of an intracellular ion well for Na^+

Studies on N790C-TMRM and L311C-TMRM clearly show a shift of the midpoint potential, $V_{0.5}$, towards more positive potentials if the internal Na^+ concentration is lowered. Decreasing the internal Na^+ concentration from above 20 mM (saturation) to below 10 mM, leads to a $V_{0.5}$-shift of +18 mV and +24 mV, respectively (Fig. 3.4B, Fig. 4.2B). This observation likely results from the presence of an internal ion well. A fraction of the potential difference between the extracellular and intracellular side of the membrane drops across the length of this narrow access channel and renders the equilibrium dissociation constants of the transported ions at the binding sites voltage-dependent. Consequently a change of electrical potential has a similar effect as a change of the ion concentration on the occupancy of the ion binding sites. This, in turn, influences the conformational equilibrium and in an electrophysiological approach a change of the ion concentration will result in a shift of the midpoint potential of the Q-V and ΔF-V relationship.

Previously, (Gadsby et al., 1993) provided electrophysiological evidence for the existence of an outward facing high-field access channel. The existence of this access channel was later also confirmed via a $[Na^+]_o$-dependent shift of the midpoint potential of VCF fluorescence data (Zifarelli, 2005). Recently, convincing structural data has been acquired that speaks for the existence of an outward facing access channel in SERCA (Olesen et al., 2007) and structural data on the Na^+,K^+-ATPase also makes the existence of the same structural feature in this ATPase likely (Morth et al., 2007).

The presence of an internal ion well is still in dispute. Some data (Or et al., 1996; Wuddel & Apell, 1995) support the existence of a shallow internal ion-well with a dielectric coefficient of about 0.25. In addition, (Holmgren & Rakowski, 2006) investigated the effect of changes in the intracellular Na^+ concentration on the voltage step-induced transient currents of the Na^+,K^+-ATPase. They observed pronounced effects of changes in $[Na^+]_i$ on the amount of the translocated charge and on the kinetics of the charge translocation which are in a very good agreement with the fluorescence data of the study at hand. Yet, they did not observe a Na^+_i-dependent shift of the midpoint potential in the Q-V relationship. As a possible explanation for this Holmgren and Rakowski propose the isolation of the intracellular ion-binding process due to the relatively slow occlusion reaction which follows ion-binding. There is, however, no obvious reason why the shift of $V_{0.5}$ might be detectable by fluorescence and not electrically. Supporting evidence for an internal access channel coming from structural data is not as clear as for the external access channel. During the pump cycle of SERCA large intracellular rearrangements of the N, P and especially the A domain are connected with extensive movements of intracellular sections of TM1-TM2 and TM3-TM4. Upon cytosolic ion binding and release, the structures adjacent to the binding sites seem to loosen up, whereas upon extracellular ion release and binding these structures seem to be packed more tightly. These features might hint at an intracellular access channel and they can also be seen as further structural indications for the alternating access model.

It has to be mentioned that the shift for E312C-TMRM is also comparable in magnitude, but directed towards more negative potentials (-23 mV). Yet, the exceptional character of residue E312 is elaborated in chapters 6.2 and 6.8 and the meaning of this observation will not be discussed further.

6.8 Residue E312 in the second extracellular loop is important for access to the ion binding sites

It was already mentioned above (chapter 6.2) that, judging from the different midpoint potentials, the introduction of the cysteine mutations for TMRM attachment has an impact on the position of the conformational equilibrium. Compared to the wild type, the equilibria of N790C and L311C are shifted towards $E_2(P)$. Interestingly, the equilibrium of E312C is shifted towards $E_1(P)$. Both the $V_{0.5}$ value determined for the translocated charge and that determined for the fluorescence of E312C-TMRM under Na^+/Na^+ exchange

conditions (-39 $\pm$ 3 mV and -27 $\pm$ 4 mV, respectively) correspond well with the value of $V_{0.5}$ determined for the Q-V relationship of this mutant (Capendeguy et al., 2006). The observation that fluorescence signals and transient currents of E312C-TMRM are mainly evoked by depolarising potentials supports the assumption of a fundamental shift of the $E_1(P)/E_2(P)$ equilibrium towards $E_1(P)$ (Fig. 5.1A).

A possible source for the explanation of this phenomenon can be found in recent structural information on various P-type ATPases. Structural data on SERCA documents the involvement of TM3-TM4 and the respective loop region in regulating ion access to and from the binding sites from the extracellular side (Olesen et al., 2007). Consequently, the elimination of a negative charge in this region might disrupt the proper function of this structural feature and change the apparent affinities for one or both translocated ion species with clear effects for the equilibrium. A reasonable explanation for the shift of the equilibrium towards $E_1(P)$ due to the introduced mutation would be an increased apparent affinity for external Na^+ as a result of the structural alteration or changes in the electrostatic landscape. Rebinding of Na^+ and the conformational transition to $E_1(P)$ would be favored. Since the apparent rate constants of the conformational change clearly show a voltage dependent increase upon progressive hyperpolarisation in spite of the small ΔF (Fig. 5.1 A and B), it can be assumed that the access channel for Na^+ rebinding is operational.

In addition, it was found for E312C-TMRM that even if an unusually high proportion of a Na^+ containing solution is substituted with potassium ($[K^+]_o$ = 50 mM), changes in fluorescence intensity upon voltage pulses can still be observed. Generally, a K^+ concentration of 10 mM or more is sufficient to thoroughly relocate the equilibrium to E_1 (see Fig. 3.5) which prevents evocable fluorescence changes in the monitored potential range. Interestingly, the K^+-dependent change of the fluorescence signals and the related shift in $V_{0.5}$ towards more positive potentials (Fig. 5.3, Fig. 5.4A and C) are similar to those previously observed in the N790C-TMRM sensor complex (Fig. 3.5, 3.6A and B). Indeed, 5-10 times higher K^+ concentrations were needed in E312C-TMRM experiments to achieve a comparable K^+ effect. Hence, our VCF measurements indicate a decreased apparent affinity for K^+ if the negative charge at position E312 is eliminated. This is in full accord with our previous assumption of an increased apparent affinity for external Na^+ since this would also lead to the requirement of higher K^+ concentrations for the progression of the cycle via the K^+ branch if Na^+ is present. The importance of the glutamate residue E312 for ion occlusion/release has previously been alluded to (Capendeguy et al., 2006) (Eguchi et al., 2005). It is however still an open question if the

effects resulting from substitution of E312 are more of a structural or more of an electrostatic nature. Interestingly, a double mutant in the TM5-TM6 loop that also eliminates a negatively charged amino acid (N790C, E779A) showed a very similar behavior in VCF experiments (Geibel, 2003). It can therefore be concluded that at least two negatively charged amino acids of two different extracellular loops are important for regulating access to the binding sites.

In summary, the work at hand shows that VCF is a powerful tool to investigate partial reactions and structural features of the Na^+,K^+-ATPase by looking at the conformational changes at selected reporter positions. It was possible to find good indications for the existence of an intracellular access channel for Na^+ and an extracellular access channel for K^+. In addition, the importance of the Na^+ and K^+ ion ratios could be elucidated, which seem to be a major determinant for the position of the conformational equilibrium. Finally, in conjunction with previous date (Geibel, 2003), the crucial role of negatively charged glutamate residues in the 2nd and 3rd extracellular loop for the control of ion-access to the binding sites could be verified.

Zusammenfassung

In der vorliegenden Arbeit wurden die Methoden der ortsspezifischen Fluoreszenzmarkierung und der Voltage Clamp Fluorometrie (VCF) kombiniert um die Konformationsänderungen der Na^+,K^+-ATPase während verschiedener elektrogener Reaktionsschritte des Pumpzyklus zu untersuchen. Neben der extrazellulären Freisetzung von Na^+ waren vor allem die interne Na^+-Bindung und externe K^+-Bindung von Interesse, da diese aufgrund ihrer geringen Elektrogenizität mit rein elektrophysiologischen Methoden nicht, oder nur ungenügend, erfasst werden können. Es sollten vor allem Informationen über die Dynamik der mit den Reaktionsschritten assoziierten Konformationsänderungen gewonnen werden und der Einfluss der Pumpsubstrate Na^+ und K^+ auf die Lage des Konformationsgleichgewichts geklärt werden.

Als Expressionssystem für die untersuchte Schaf-Na^+,K^+-ATPase α_1–Untereinheit wurden *Xenopus laevis* Oozyten gewählt. Die eingeführten Cysteinmutationen N790C (Loopregion zwischen den Transmembranhelices TM5-TM6), sowie L311C und E312C (Loopregion TM3-TM4) binden den Fluoreszenzfarbstoff TMRM (Tetramethylrhodamin-6-maleimid) und bilden einen Sensorkomplex, mit dem Konformationsänderungen des Enzyms aufgrund von Hydrophobizitätsänderungen in der Umgebung des Farbstoffs detektiert werden können.

Die kürzlich verfügbare Röntgenstruktur der Na^+,K^+-ATPase und eine auf verschiedenen Röntgenstrukturen basierende Simulation des Pumpzyklus der verwandten P-Typ ATPase SERCA konnten gute Informationen über die in dieser Studie ausgewählten Sensorpositionen liefern. Das an ein Cystein gekoppelte Reporterfluorophor TMRM befindet sich sowohl in der hauptsächlich untersuchten Position N790C als auch in den Positionen L311C und E312C am äußeren Ende einer Struktur, die höchstwahrscheinlich einen externen Zugangskanal oder „access channel" zu den Ionenbindungsstellen darstellt. Beim Austritt der drei Na^+-Ionen nach dem $E_1(P)/E_2(P)$ Übergang wird dieser Kanal geöffnet wobei er nach der Bindung bzw. vor dem Austritt der zwei K^+-Ionen auf der Innenseite (beim E_2/E_1 Übergang) wieder geschlossen wird. Beim Öffnen und Schließen des Kanals ergeben sich durch die auftretenden Konformationsänderungen Hydrophobizitätesunterschiede in der Umgebung des gekoppelten Fluorophors, die sich jeweils in einer sich verändernden Fluoreszenzintensität widerspiegeln. Somit sind die

beobachteten Fluoreszenzänderungen direkt an die Übergänge zwischen den wichtigsten Enzymkonformationen des Pumpzyklus ($E_1(P)/E_2(P)$-Übergang und E_2/E_1-Übergang) gekoppelt.

Eine Analyse der Relaxationskinetiken der Fluoreszenzantworten liefert Informationen über die Spannungsabhängigkeit und/oder die Substrat-konzentrationsabhängigkeit der Zeitkonstanten der beobachteten Konformationsänderung. Hier zeigten sich schon in früheren Experimenten große Parallelen zum Verhalten der Zeitkonstanten des assoziierten Ladungstransports. Weiterhin lässt sich aus den Sättigungswerten der Fluoreszenzrelaxationen auch die Position des Konformationsgleichgewichts bestimmen. Diese Möglichkeit besteht, weil die durch Spannungssprünge verschobene Ladung Q und die begleitenden Fluoreszenz-sättigungswerte ΔF praktisch identische sigmoide Spannungsabhängigkeiten aufweisen, welche für Q bekanntermaßen das $E_1(P)/E_2(P)$ Verhältnis bzw. das E_1/E_2 Verhältnis wiedergeben. Da die Fluoreszenzinformation der elektrischen Information praktisch äquivalent ist, können über die ΔF-V Beziehung somit auch Aussagen über Gleichgewichtsverschiebungen und die transportierte Ladung getroffen werden

Um Informationen über die interne Na^+-Bindung und der externen K^+-Bindung zu erhalten, wurden vorrangig die Auswirkungen der intrazellulären Na^+-Konzentration und der extrazellulären K^+-Konzentration auf die Kinetiken der beobachteten Fluoreszenzrelaxationen und das Konformationsgleichgewicht der Mutante N790C untersucht. Dazu war es notwendig, neben den leicht zu manipulierenden extrazellulären Ionenkonzentrationen auch die Konzentration des intrazellulären Na^+ zu kontrollieren. Um dies zu erreichen wurde der epitheliale Natriumkanal (ENaC) zusammen mit der Na^+,K^+-ATPase koexprimiert. EnaC kann bei nach außen gerichteten Na^+-Konzentrationsgradienten zur Senkung des internen Na^+-Gehalts der Zelle verwendet werden. Anschließend ist durch den spezifisch und reversibel an EnaC bindenden Blocker Amilorid eine schrittweise Erhöhung der Na^+-Konzentration bei nach innen gerichteten Na^+-Konzentrationsgradienten möglich.

Weiterhin wurden Untersuchungen der Sensorpositionen L311C und E312C in der Loop-Region TM3-TM4 durchgeführt. Hierbei stand besonders die Position E312C im Mittelpunkt des Interesses, da aufgrund der Eliminierung einer negativen Ladung in der Nähe des „access channels" mit einer veränderten der Na^+,K^+-ATPase Charakteristik gerechnet werden konnte.

Die schrittweise Erhöhung der internen Na^+-Konzentration nach vorhergehender Verringerung auf c.a. 1 mM bewirkt eine deutliche, graduelle Veränderung der Spannungsabhängigkeit der Fluoreszenzrelaxationen des N790C-TMRM Sensorkomplexes. Bei sehr niedrigen Na^+-Konzentrationen können nur depolarisierende Spannungssprünge Fluoreszenzrelaxationen hervorrufen, wohingegen unter sättigenden Na^+-Bedingungen fast ausschließlich hyperpolarisierende Spannungssprünge dazu in der Lage sind. Da unter den gewählten Na^+/Na^+-Austauschbedingungen depolarisierende Spannungssprünge das Gleichgewicht nach $E_2(P)$ verschieben und hyperpolarisierende nach $E_1(P)$, kann daraus geschlossen werden, dass sich das Konformationsgleichgewicht bei steigender Na^+-Konzentration von $E_1(P)$ nach $E_2(P)$ verlagert. Aufgrund der generell sehr langsam verlaufenden Konformationsänderung des N790C-TMRM Sensorkomplexes lassen sich keine definitiven Aussagen über Einflüsse der Na^+-Konzentration auf die Dynamik des Prozesses treffen. Es ist jedoch ersichtlich, dass die apparente translozierte Ladung mit sinkender Konzentration deutlich abnimmt.

Substituiert man bei sättigender interner Na^+-Konzentration einen Teil des externen Na^+ mit K^+, so ist eine gegenläufige Entwicklung, also eine Verlagerung des Konformationsgleichgewichts von E_2 nach E_1 zu beobachten. Im Gegensatz zum oben beschriebenen Experiment in dem das Konformationsgleichgewicht per Spannungssprung nur über den Na^+-Zweig zwischen $E_1(P)$ und $E_2(P)$ verschoben werden konnte, gewinnt in Gegenwart von K^+ der K^+-Zweig mit steigender Konzentration zunehmend an Gewicht, bis das Gleichgewicht bei sättigender K^+-Konzentration vollends von E_2 nach E_1 verschoben ist. Die zunehmende Bedeutung das K^+-Zweigs lässt sich auch anhand des $E_2(P)/E_1(P)$ Übergangs bei Hyperpolarisation veranschaulichen. Dieser wird in Abwesendheit von K^+ aufgrund des „access channels" für Na^+ deutlich beschleunigt. Mit zunehmender K^+-Konzentration verliert sich aber diese spannungsabhängige Beschleunigung, was darauf hinweist, dass dieser Prozess schrittweise durch den vermutlich weitaus weniger spannungsabhängigen E_2/E_1-Übergang des K^+-Zweigs abgelöst wurde. Dies spiegelte sich auch in der Abnahme der apparenten translozierten Ladung wieder.

Wird extrazellulär vorhandenes Na^+ durch das nicht von der Pumpe umgesetzte NMG^+ ersetzt, so lässt sich auch eine Verschiebung des Gleichgewichts nach E_1 beobachten, jedoch ist die benötigte Menge an K^+ für eine vergleichbare Verschiebung deutlich reduziert. Die praktisch potentialunabhängigen Geschwindigkeitskonstanten der Fluoreszenzrelaxationen unter diesen Bedingungen zeigen, dass keine Na^+-Rückbindung durch Hyperpolarisation erfolgen kann. Jegliche hierdurch hervorgerufenen

Fluoreszenzsignale müssten somit mit einer spannungsabhängigen Konformationsänderung im K^+-Zweig begründet werden. Fluoreszenzänderungen aufgrund depolarisierender Spannungssprünge könnten aber sowohl durch den E_1/E_2 Übergang des K^+-Zweigs oder den $E_1(P)/E_2(P)$ Übergang des Na^+-Zweigs hervorgerufen werden. Die K^+-abhängige Abnahme der apparenten translozierten Ladung verläuft ähnlich wie in Gegenwart von K^+, jedoch sind auch hierfür wesentlich geringere Konzentrationen notwendig.

Interessanterweise lassen sich durch geringe interne Na^+-Konzentrationen und erhöhte externe K^+-Konzentrationen Gleichgewichtseinstellungen erreichen, die eine praktisch identische Spannungsabhängigkeit aufweisen. Weil sich die Zeitkonstanten der Fluoreszenzrelaxationen in Geschwindigkeit und Spannungsabhängigkeit unterscheiden, ist die Zugehörigkeit zu verschiedenen Zweigen des Reaktionszyklus klar ersichtlich. Da in beiden Fällen Spannung und Konzentration vergleichbar auf die Ionenbindung und somit das Gleichgewicht einwirken, kann von der Existenz eines tiefen Ionenschachts (high-field access channel, ion well) sowohl für internes Na^+ als auch für externes K^+ ausgegangen werden. Weiterhin lässt sich sowohl für geringe interne Na^+-Konzentration als auch für erhöhte externe K^+-Konzentration eine Abnahme der apparenten translozierten Ladung beobachten, welche vermutlich auf die geringe Elektrogenizität der assoziierten Prozesse (interne Na^+-Bindung, externe K^+-Bindung) zurückzuführen ist.

Die Untersuchung der Sensorpositionen L311C und E312C des zweiten extrazellulären Loops zeigte, dass beide Positionen eine gute Übereinstimmung der Q-V und ΔF-V Kurven aufweisen und somit analog der Position N790C in VCF-Experimenten verwendet werden können.

Beide Positionen weisen deutlich schnellere Fluoreszenzrelaxationen als N790C auf, was kinetische Untersuchungen vereinfacht. Das Mittelpunktspotential der ΔF-V bzw. Q-V Verteilungen weist auf ein Konformationsgleichgewicht hin, das für L311C weniger nach $E_2(P)$ verschoben ist als für N790C. Das Gleichgewicht von E312C war jedoch deutlich nach $E_1(P)$ verschoben, so dass hauptsächlich depolarisierende Spannungssprünge zu Fluoreszenzantworten führten.

Untersuchungen bei unterschiedlichen internen Na^+-Konzentration zeigen, dass sich der L311C-TMRM Sensorkomplex tendenziell sehr ähnlich wie der N790C-TMRM Sensorkomplex verhält. Durch die im Vergleich zu N790C-TMRM beschleunigten Fluoreszenzrelaxationen kann eine Verlangsamung der Konformationsänderung bei niedrigen Na^+-Konzentrationen anhand von L311C-TMRM wesentlich besser aufgezeigt werden. Auffällig ist jedoch die extreme Verlangsamung des Prozesses bei sehr niedrigen

internen Na$^+$-Konzentrationen. Interessanterweise kann auch keine konzentrationsabhängige Veränderung der apparenten translozierten Ladung festgestellt werden. Da durch die eingeführte Mutation keine geladene oder besonders große Aminosäure substituiert wurde, gibt es momentan für diesen Befund noch keine nahe liegende Erklärung.

Der E312C-TMRM Komplex zeigt ebenfalls deutlich, wie sich die Relaxationskinetiken verlangsamen wenn die interne Na$^+$-Konzentration verringert wird. Da Fluoreszenzsignale fast ausschließlich als Antwort auf depolarisierende Potentialsprünge auftreten kann daraus geschlossen werden, dass das Gleichgewicht generell stark auf die Seite von E$_1$(P) verlagert ist. Dies könnte mit einer gesteigerten Affinität der Mutante für externes Na$^+$ erklärt werden, da die hierdurch verstärkte Na$^+$-Rückbindung den E$_2$(P)/E$_1$(P) Übergang favorisieren würde. Es kann eine deutliche Beschleunigung der Relaxationskinetiken bei Hyperpolarisierung beobachtet werden, welche zumindest dafür spricht, dass der Zugangskanal für externes Na$^+$ funktionstüchtig ist. Eine gesteigerte Affinität für externes Na$^+$ würde auch erklären, warum fünf- bis zehnfach höhere K$^+$-Konzentrationen im Falle von E312C-TMRM nötig sind, um Fluoreszenzantworten zu erzeugen, die mit denen des Sensorkomplexes N790C-TMRM in Präsenz von K$^+$ vergleichbar sind. In einer anderen VCF-Studie zeigte eine Doppelmutante, bei der ebenfalls ein Glutamatrest eliminiert wurde (N790C, E779A), eine vergleichbar verringerte apparente Affinität für K$^+$. Diese Beobachtung hebt die große Bedeutung negativ geladener Aminosäuren im Bereich des Zugangskanals deutlich hervor.

Bibliography

Albers, R.W. 1967. Biochemical aspects of active transport. *Annu Rev Biochem* **36:**727-56

Apell, H.J. 2004. How do P-type ATPases transport ions? *Bioelectrochemistry* **63:**149-56

Aperia, A. 2007. New roles for an old enzyme: Na,K-ATPase emerges as an interesting drug target. *J Intern Med* **261:**44-52

Artigas, P., Gadsby, D.C. 2003. Na+/K+-pump ligands modulate gating of palytoxin-induced ion channels. *Proc Natl Acad Sci U S A* **100:**501-5

Bahinski, A., Nakao, M., Gadsby, D.C. 1988. Potassium translocation by the Na+/K+ pump is voltage insensitive. *Proc Natl Acad Sci U S A* **85:**3412-6

Barwe, S.P., Kim, S., Rajasekaran, S.A., Bowie, J.U., Rajasekaran, A.K. 2007. Janus model of the Na,K-ATPase beta-subunit transmembrane domain: distinct faces mediate alpha/beta assembly and beta-beta homo-oligomerization. *J Mol Biol* **365:**706-14

Borlinghaus, R., Apell, H.J., Lauger, P. 1987. Fast charge translocations associated with partial reactions of the Na,K-pump: I. Current and voltage transients after photochemical release of ATP. *J Membr Biol* **97:**161-78

Buhler, R., Sturmer, W., Apell, H.J., Lauger, P. 1991. Charge translocation by the Na,K-pump: I. Kinetics of local field changes studied by time-resolved fluorescence measurements. *J Membr Biol* **121:**141-61

Capendeguy, O., Chodanowski, P., Michielin, O., Horisberger, J.D. 2006. Access of extracellular cations to their binding sites in Na,K-ATPase: role of the second extracellular loop of the alpha subunit. *J Gen Physiol* **127:**341-52

Cha, A., Bezanilla, F. 1997. Characterizing voltage-dependent conformational changes in the Shaker K+ channel with fluorescence. *Neuron* **19:**1127-40

Crambert, G., Hasler, U., Beggah, A.T., Yu, C., Modyanov, N.N., Horisberger, J.D., Lelievre, L., Geering, K. 2000. Transport and pharmacological properties of nine different human Na, K-ATPase isozymes. *J Biol Chem* **275:**1976-86

De Weer, P., Gadsby, D.C., Rakowski, R.F. 2001. Voltage dependence of the apparent affinity for external Na(+) of the backward-running sodium pump. *J Gen Physiol* **117:**315-28

Dempski, R.E., Friedrich, T., Bamberg, E. 2005. The beta subunit of the Na+/K+-ATPase follows the conformational state of the holoenzyme. *J Gen Physiol* **125:**505-20

Dempski, R.E., Lustig, J., Friedrich, T., Bamberg, E. 2008. Structural arrangement and conformational dynamics of the gamma subunit of the Na+/K+-ATPase. *Biochemistry* **47:**257-66

Domaszewicz, W., Apell, H. 1999. Binding of the third Na+ ion to the cytoplasmic side of the Na,K-ATPase is electrogenic. *FEBS Lett* **458:**241-6

Eguchi, H., Takeda, K., Schwarz, W., Shirahata, A., Kawamura, M. 2005. Involvement in K+ access of Leu318 at the extracellular domain flanking M3 and M4 of the Na+,K+-ATPase alpha-subunit. *Biochem Biophys Res Commun* **330:**611-4

Friedrich, T., Nagel, G. 1997. Comparison of Na+/K(+)-ATPase pump currents activated by ATP concentration or voltage jumps. *Biophys J* **73:**186-94

Gadsby, D.C., Nakao, M., Bahinski, A. 1989. Voltage dependence of transient and steady-state Na/K pump currents in myocytes. *Mol Cell Biochem* **89:**141-6

Gadsby, D.C., Rakowski, R.F., De Weer, P. 1993. Extracellular access to the Na,K pump: pathway similar to ion channel. *Science* **260:**100-3

Geering, K. 2005. Function of FXYD proteins, regulators of Na, K-ATPase. *J Bioenerg Biomembr* **37:**387-92

Geibel, S. 2003. Elektrophysiologische Charakterisierung der Konformationsdynamik von Ionenpumpen in situ. pp. 190. Johann Wolfgang Goethe Universität, Frankfurt am Main

Geibel, S., Kaplan, J.H., Bamberg, E., Friedrich, T. 2003. Conformational dynamics of the Na+/K+-ATPase probed by voltage clamp fluorometry. *Proc Natl Acad Sci U S A* **100:**964-9

Hasler, U., Wang, X., Crambert, G., Beguin, P., Jaisser, F., Horisberger, J.D., Geering, K. 1998. Role of beta-subunit domains in the assembly, stable expression, intracellular routing, and functional properties of Na,K-ATPase. *J Biol Chem* **273:**30826-35

Holmgren, M., Rakowski, R.F. 2006. Charge translocation by the Na+/K+ pump under Na+/Na+ exchange conditions: intracellular Na+ dependence. *Biophys J* **90:**1607-16

Horisberger, J.D. 2004. Recent insights into the structure and mechanism of the sodium pump. *Physiology (Bethesda)* **19:**377-87

Horisberger, J.D., Kharoubi-Hess, S. 2002. Functional differences between alpha subunit isoforms of the rat Na,K-ATPase expressed in Xenopus oocytes. *J Physiol* **539:**669-80

Horisberger, J.D., Kharoubi-Hess, S., Guennoun, S., Michielin, O. 2004. The fourth transmembrane segment of the Na,K-ATPase alpha subunit: a systematic mutagenesis study. *J Biol Chem* **279:**29542-50

Humphrey, W., Dalke, A., Schulten, K. 1996. VMD: visual molecular dynamics. *J Mol Graph* **14:**33-8, 27-8

Jasti, J., Furukawa, H., Gonzales, E.B., Gouaux, E. 2007. Structure of acid-sensing ion channel 1 at 1.9 A resolution and low pH. *Nature* **449:**316-23

Jewell, E.A., Lingrel, J.B. 1991. Comparison of the substrate dependence properties of the rat Na,K-ATPase alpha 1, alpha 2, and alpha 3 isoforms expressed in HeLa cells. *J Biol Chem* **266:**16925-30

Jorgensen, P.L., Hakansson, K.O., Karlish, S.J. 2003. Structure and mechanism of Na,K-ATPase: functional sites and their interactions. *Annu Rev Physiol* **65:**817-49

Kaplan, J.H. 2005. A moving new role for the sodium pump in epithelial cells and carcinomas. *Sci STKE* **2005:**pe31

Karlish, S.J., Yates, D.W. 1978. Tryptophan fluorescence of (Na+ + K+)-ATPase as a tool for study of the enzyme mechanism. *Biochim Biophys Acta* **527:**115-30

Keenan, S.M., DeLisle, R.K., Welsh, W.J., Paula, S., Ball, W.J., Jr. 2005. Elucidation of the Na+, K+-ATPase digitalis binding site. *J Mol Graph Model* **23:**465-75

Lauger, P., Apell, H.J. 1988. Voltage dependence of partial reactions of the Na+/K+ pump: predictions from microscopic models. *Biochim Biophys Acta* **945:**1-10

Li, C., Capendeguy, O., Geering, K., Horisberger, J.D. 2005. A third Na+-binding site in the sodium pump. *Proc Natl Acad Sci U S A* **102:**12706-11

Lutsenko, S., Anderko, R., Kaplan, J.H. 1995. Membrane disposition of the M5-M6 hairpin of Na+,K(+)-ATPase alpha subunit is ligand dependent. *Proc Natl Acad Sci U S A* **92:**7936-40

Mannuzzu, L.M., Moronne, M.M., Isacoff, E.Y. 1996. Direct physical measure of conformational rearrangement underlying potassium channel gating. *Science* **271:**213-6

Morth, J.P., Pedersen, B.P., Toustrup-Jensen, M.S., Sorensen, T.L., Petersen, J., Andersen, J.P., Vilsen, B., Nissen, P. 2007. Crystal structure of the sodium-potassium pump. *Nature* **450:**1043-9

Nakao, M., Gadsby, D.C. 1986. Voltage dependence of Na translocation by the Na/K pump. *Nature* **323:**628-30

Nakao, M., Gadsby, D.C. 1989. [Na] and [K] dependence of the Na/K pump current-voltage relationship in guinea pig ventricular myocytes. *J Gen Physiol* **94:**539-65

Ogawa, H., Toyoshima, C. 2002. Homology modeling of the cation binding sites of Na+K+-ATPase. *Proc Natl Acad Sci U S A* **99:**15977-82

Olesen, C., Picard, M., Winther, A.M., Gyrup, C., Morth, J.P., Oxvig, C., Moller, J.V., Nissen, P. 2007. The structural basis of calcium transport by the calcium pump. *Nature* **450:**1036-42

Or, E., Goldshleger, R., Karlish, S.J. 1996. An effect of voltage on binding of Na+ at the cytoplasmic surface of the Na(+)-K+ pump. *J Biol Chem* **271:**2470-7

Pavlov, K.V., Sokolov, V.S. 2000. Electrogenic ion transport by Na+,K+-ATPase. *Membr Cell Biol* **13:**745-88

Post, R.L., Hegyvary, C., Kume, S. 1972. Activation by adenosine triphosphate in the phosphorylation kinetics of sodium and potassium ion transport adenosine triphosphatase. *J Biol Chem* **247:**6530-40

Rakowski, R.F. 1993. Charge movement by the Na/K pump in Xenopus oocytes. *J Gen Physiol* **101:**117-44

Rakowski, R.F., Gadsby, D.C., De Weer, P. 1997. Voltage dependence of the Na/K pump. *J Membr Biol* **155:**105-12

Reyes, N., Gadsby, D.C. 2006. Ion permeation through the Na+,K+-ATPase. *Nature* **443:**470-4

Rossier, B.C. 2003. The epithelial sodium channel (ENaC): new insights into ENaC gating. *Pflugers Arch* **446:**314-6

Skou, J.C. 1957. The influence of some cations on an adenosine triphosphatase from peripheral nerves. *Biochim Biophys Acta* **23:**394-401

Sturmer, W., Apell, H.J., Wuddel, I., Lauger, P. 1989. Conformational transitions and change translocation by the Na,K pump: comparison of optical and electrical transients elicited by ATP-concentration jumps. *J Membr Biol* **110:**67-86

Tanford, C. 1982. Simple model for the chemical potential change of a transported ion in active transport. *Proc Natl Acad Sci U S A* **79:**2882-4

Toyoshima, C., Mizutani, T. 2004. Crystal structure of the calcium pump with a bound ATP analogue. *Nature* **430:**529-35

Weber, W. 1999. Ion currents of Xenopus laevis oocytes: state of the art. *Biochim Biophys Acta* **1421:**213-33

Wuddel, I., Apell, H.J. 1995. Electrogenicity of the sodium transport pathway in the Na,K-ATPase probed by charge-pulse experiments. *Biophys J* **69:**909-21

Zifarelli, G. 2005. Electrophysiological and spectroscopical characterization of the Na,K-ATPase. *In:* Chemische und Pharmazeutische Wissenschaften. pp. 189. Johann Wolfgang Goethe Universität, Frankfurt am Main

Danksagung

Mein herzlichster Dank gilt Herrn Prof. Dr. Ernst Bamberg, der mich großzügig und verständnisvoll unterstützt und betreut hat. Die vielen Diskussionen mit ihm haben wesentlich zum Gelingen dieser Arbeit beigetragen.

Herrn Prof. Dr. Thomas Friedrich danke ich für die Einführung in das Thema „Voltage-Clamp Fluorometry" und die verwendeten Techniken sowie für die Bereitstellung der bearbeiteten Mutanten.

Herrn Dr. Robert Dempski und Herrn Dr. Dirk Zimmermann möchte ich herzlich für ihre stete Diskussionsbereitschaft danken. Ihre Bereitschaft, stets „KnowHow" bezüglich der „Voltage Clamp Fluorometry" an mich weiterzugeben, haben mir zudem bei der Datenanalyse viel geholfen. Auch Herrn Prof. Dr. Klaus Fendler, Herrn Dr. Jürgen Rettinger, Herrn Dr. Klaus Hartung und Frau Dr. Sonja Kleinlogel möchte ich für ihre stete Diskussionsbereitschaft danken.

Bei Dr. Luis Beaugé bedanke ich mich für seine Unterstützung bei der Entwicklung von Simulationen des Pumpzyklus der Na^+,K^+-ATPase.

Prof. Dr. Georg Nagel möchte ich für die Bereitstellung des epithelialen Na^+-Kanals EnaC danken.

Großer Dank gilt auch den technischen Assistentinnen Frau Janna Lustig und Frau Verena Pintschovius für Ihre großartige Unterstützung im Labor.

Mein herzlicher Dank gilt allen Kollegen der Arbeitsgruppe Bamberg die im Labor – und darüber hinaus – stets eine freundschaftliche Atmosphäre geschaffen haben, was sich sehr positiv auf die Arbeit auswirkte. Besonders möchte ich auch Frau Heidi Bergemann für ihr unermüdliches Engagement und Ihre Hilfsbereitschaft in allen Lebenslagen danken.

Auch meinen Eltern möchte ich für ihre Freundschaft und Unterstützung herzlich danken.

Lebenslauf

Name:	Stefan Geys
Geburtsdatum/-Ort:	7. März 1975 in Würzburg

Schulausbildung

1981-1985	Volksschule Gerbrunn (Eichendorffschule)
1985-1994	Städt. Schönborngymnasium Würzburg, Abschluss Abitur

Ausbildung

1994-2000	Studium der Biologie (Diplom) an der Bayerischen Julius-Maximilians - Universität Würzburg; Hauptfach Biotechnologie Thema der Diplomarbeit: „Untersuchung eines spezifischen Porins von *Pseudomonas aeruginosa*". Betreuer: Prof. Dr. R. Benz.
2000-2002	Studium an der Graduate School of Biomedical Sciences, Health Science Center, Texas A&M University, USA Forschungsthema: "Investigation of gating in the channel forming protein α-hemolysin using covalently attached polymers". Betreuer: Prof. J.H.P. Bayley
2002-heute	Promotion am Max Planck Institut für Biophysik, Frankfurt am Main Thema der Dissertation: „Substrate-Dependent Effects on the Conformational Equilibrium of the Na^+,K^+-ATPase monitored by VCF". Betreuer: Prof. Dr. E. Bamberg

Publikationen

Geys, S., Dempski, R.E., Bamberg, E.
   Substrate-Dependent Effects on the Conformational Equilibrium of the Na^+,K^+-ATPase monitored by Voltage Clamp Fluorometry (in preparation)